Coordination Chemistry Reviews, 95 (1989) 239–294
Elsevier Science Publishers B.V., Amsterdam – Printed in The Netherlands

ELECTROCHEMICAL STUDIES OF RUTHENIUM COMPOUNDS PART I. LIGAND OXIDATION LEVELS

BARINDRA KUMAR GHOSH and ANIMESH CHAKRAVORTY *

Department of Inorganic Chemistry, Indian Association for the Cultivation of Science, Calcutta 700 032 (India)

(Received 17 October 1988)

CONTENTS

---

* Author to whom correspondence should be addressed.

0010-8545/89/$19.60

ABBREVIATIONS

Symbols

E	variable potential
$E_{1/2}$	polarographic half-wave potential
E_T°	formal potential at temperature T
$E^\circ(x)$	formal potential of the couple in eqn. (x)
E_{pa}	anodic peak potential in cyclic voltammetry
E_{pc}	cathodic peak potential in cyclic voltammetry
$\overline{E}_p$	average of cathodic and anodic peak potentials in cyclic voltammetry
ΔE_p	peak-to-peak separation in cyclic voltammetry
$+\cdot$	cation radical

$-\bullet$	anion radical
ν_{CT}	charge transfer maximum

Solvents

dce	1,2-dichloroethane
dcm	dichloromethane
dmf	*N*, *N*-dimethylformamide
dmso	dimethyl sulphoxide
MeCN	acetonitrile
py	pyridine

Supporting electrolytes

tbab	tetra-*n*-butylammonium tetrafluoroborate
tbah	tetra-*n*-butylammonium hexafluorophosphate
tbai	tetra-*n*-butylammonium iodide
tbap	tetra-*n*-butylammonium perchlorate
teah	tetraethylammonium hexafluorophosphate
teap	tetraethylammonium perchlorate
tpap	tetra-*n*-propylammonium perchlorate

A. PREAMBLE

(i) Introduction

In many ways the chemistry of transition metals is the chemistry of multiple oxidation states and the associated redox phenomena. If a particular element were to be singled out to illustrate this viewpoint, a model choice would be ruthenium—an element that is directly or indirectly the active centre of a plethora of redox phenomena encompassing ten different oxidation states and a breathtaking diversity of structure and bonding.

Recent advances in electronic instrumentation and pragmatic theories have made available to chemists powerful electrochemical tools for fine probing of redox changes executed in electrochemical cells in a controlled manner [1–7]. The impact of these developments has been felt in many areas of chemistry [8–12]. The chemistry of ruthenium, which has witnessed spectacular progress [13–15] in recent years, is an example per se. The purpose of this article is to highlight certain advances in ruthenium chemistry brought about through application of electrochemical techniques.

(ii) *Early history*

Jaroslav Heyrovský of Prague invented polarography in 1922. In the first three decades of polarography, very few studies were made on ruthenium compounds. The status is adequately reviewed in a 1951 paper dealing with the polarography of ruthenium(IV) in perchloric acid solution [16]. Metallocenes were discovered at about this time and the first report on the polarography of ruthenocene appeared in 1952 [17]. The main conclusion of this report, i.e. the oxidation of $[Ru^{II}(\eta^5\text{-}C_5H_5)_2]$ to $[Ru^{III}(\eta^5\text{-}C_5H_5)_2]^+$, has, however, proved to be erroneous; the electrode material (mercury) is actually oxidized [18]. Definitive studies of early years concern cyano [19], oxo [20] and gluconato [21] species. The total volume of information available on the polarography of ruthenium complexes was still very meagre in 1960. Indeed, widespread use of voltammetric techniques in ruthenium chemistry began after 1970. Since then the modern techniques have become routinely available and subsequent progress has been rapid.

(iii) *Electrochemical techniques*

The information content is large and the uses of electrochemical experiments are many [4,5]. Table 1 lists some of the types of studies carried out by coordination chemists using electrochemical methods.

The principles of the various controlled-potential and controlled-current electrochemical techniques now available to chemists are excellently covered in several texts [1,5,7]. Practical details of cells, electrodes, solvents and supporting electrolytes are also available [3,4,9]. Coordination chemists commonly use polarography at dropping mercury and rotating solid electrodes, cyclic voltammetry, differential pulse voltammetry, alternating cur-

TABLE 1

Some types of studies

A. Accessible electron transfer steps:
    (a) metal and ligand oxidation levels
    (b) electron stoichiometry
    (c) reduction potential and its correlation with other properties
    (d) reversibility and heterogeneous kinetics
B. Chemical reactions induced by electrochemical electron transfer
C. Excited state redox properties
D. Electrosynthesis
E. Chemistry with modified electrode

rent voltammetry and constant potential coulometry. Undoubtedly the most popular technique today is cyclic voltammetry at stationary solid electrodes. This technique was first practised by Sevcik in the late forties [22].

(iv) Scope

In the present review we shall be primarily concerned with the oxidation states (see item A in Table 1) of certain ligands coordinated to ruthenium. This choice is deliberate since this is one area where the unique power of electrochemical methods is splendidly revealed. Without these methods, development in this area would have been greatly hampered. A brief summary of metal oxidation states is also included as a prelude to the main subject of this review. We plan to describe the details of metal oxidation levels and reactions induced by electrochemical electron transfer in future reviews. We shall generally emphasize the information derived which is of chemical interest, leaving the details of formal electrochemical arguments in the background. This work neither is nor was intended to be an exhaustive compendium of electrochemical data of ruthenium compounds.

(v) Electrode reaction and reference electrodes

Electrode reactions will be uniformly written as reductions (eqn. (1)):

$$\text{ox} + n\text{e} \rightleftharpoons \text{red} \tag{1}$$

Correspondingly, electrode potentials (E°_T) are given as reduction potentials. The saturated calomel electrode (SCE) is probably the most widely used reference electrode and all potentials in this article are referenced to SCE. The potentials of some other standards on the SCE scale at 298 K are as follows: normal hydrogen electrode (NHE), -0.242 V; saturated silver–silver chloride electrode (Ag–AgCl), -0.045 V; saturated sodium chloride calomel electrode (SSCE), -0.005 V; ferrocenium–ferrocene (Fc^+/Fc) standard [23], 0.158 V. For convenience, certain symbols and abbreviations pertaining to electrochemical studies are listed at the beginning of this review.

B. SITE OF ELECTRON TRANSFER

(i) Redox orbital

In an electrochemical redox experiment, electrons are usually transferred heterogeneously between the electrode surface and the dissolved electroactive substance, in the present case, a ruthenium complex. We consider the two cases stated in eqns. (2) and (3):

$$\mathrm{RuL} + e^- \longrightarrow \boxed{\mathrm{Ru}}\mathrm{L} \quad (2)$$

$$\mathrm{RuL} + e^- \longrightarrow \mathrm{Ru}\boxed{\mathrm{L}} \quad (3)$$

where L is a general ligand. In each case the box schematically represents the primary nature of the redox orbital, i.e. the orbital occupied by the transferred electron. The orbital is essentially metal in character in eqn. (2) and ligand in character in eqn. (3). The oxidation state of the metal changes in eqn. (2) while that of the ligand changes in eqn. (3).

Electrochemical results alone can give some indications about the redox orbitals of a particular electrogenerated species. However, collective application of spectroscopic and magnetic methods in conjunction with electrochemical techniques provides the most convincing diagnosis of the nature of such orbitals. Nitrosyl complexes of ruthenium provide good examples [24–27]. The complexes $[\mathrm{Ru(bpy)_2(NO)X}]^{z+}$ (bpy = 2,2′-bipyridine; X = N_3^-, Cl^-, NO_2^- with $z = 2$; X = NH_3, py, MeCN with $z = 3$) undergo a reversible one-electron reduction in the potential range 0.1–0.6 V in MeCN. By collective application of IR, EPR, electron spectroscopy for chemical analysis (ESCA), Mössbauer, spectral and electrochemical studies, it has been demonstrated that the site of reduction in eqn. (4) is largely π^*(NO) in character:

$$[\mathrm{Ru^{II}}\text{—}(\mathrm{NO^+})] + e^- \rightleftharpoons \left[\mathrm{Ru^{II}}(\dot{\mathrm{N}}\mathrm{O})\right] \quad (4)$$

There is, however, substantial $d\pi$(Ru)-to-π^*(NO) backbonding. There is also a nearly linear correlation between ν(NO) and E°_{298}. A reduced complex $[\mathrm{Ru(bpy)_2(NO)Cl}]\mathrm{I}$ has been isolated in pure form [24].

(ii) Redox series

Ruthenium is richly endowed with redox orbitals and it accordingly displays a large number of oxidation states. When the metal is bonded to a non-innocent ligand system which is also rich in redox orbitals, we have in principle a situation where a series of discrete electron-transfer steps could occur. Several redox series [28] of this type are well documented in ruthenium chemistry. In voltammetric experiments a redox series is expressed in the form of a sequence of redox responses. Since it is easy to control the potential of the working electrode finely (±5 mV and better), even closely spaced members of a redox series can be generated selectively in a manner that no chemical method can match.

(iii) Extreme delocalization: the case of dithiolenes

In certain instances it may be very difficult to assign individual oxidation states to the metal and ligand owing to extreme delocalization of the redox orbitals over the entire metal–ligand (ML) frame. The dithiolenes are examples per se of this situation [29,30]. Thus in $[Ru(PPh_3)(S_2C_2(CF_3)_2)_2]$ [31] the formal metal oxidation state can be 0–4 depending on how the bound ligand is formulated (**1**–**3**).

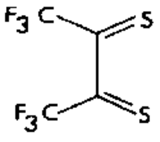

1

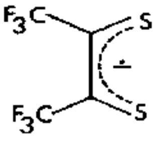

2

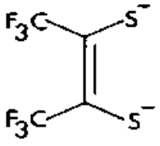

3

The complex displays a one-electron reduction wave ($E°$, ca. 0.2 V) but the redox orbital remains undefined.

C. SUMMARY OF RUTHENIUM OXIDATION STATES

(i) Classification

Ruthenium spans all oxidation states in the range -2 to $+8$ with the exception of -1 [13]. It is convenient to classify the ten observed oxidation levels in the three-tier scale as high, medium and low on the basis of their degree of oxidation. In terms of the number of known compounds and the amount of available chemistry, a second three-tier classification can be made: uncommon, common and very common. These classifications are set out in Table 2. The two very common oxidation states belong to the medium level while the high and very low (-2) oxidation states are uncommon.

(ii) High states

High oxidation levels occur in oxo complexes in which the strong σ- and π-donor abilities of O^{2-} are undoubtedly utilized. The triad RuO_4, RuO_4^- and RuO_4^{2-} (or $RuO_3(OH)_2^{2-}$) constitutes a good redox series [20,32]. Apart from RuO_4^{2-}, the hexavalent state is represented by an increasing number of complexes of the RuO_2^{2+} moiety. Similarly, more and more complexes of the monooxo radical RuO^{2+} containing the intermediate oxidation state $+4$ are being discovered. The electrochemistry of the oxo complexes is of current interest in relation to their role in oxo transfer reactions. The interrelationship of oxo, hydroxo and aquo complexes vis-à-vis ruthenium oxidation states is stated in eqns. (5) and (6) [33]:

TABLE 2

Classification of metal oxidation states

A. Degree of oxidation	
(a) High	+5, +6, +7, +8
(b) Medium	+2, +3, +4
(c) Low	−2, 0, +1
B. Occurrence	
(a) Uncommon	−2, +5, +6, +7, +8
(b) Common	0, +1, +4
(c) Very common	+2, +3

$$[\mathrm{Ru^{IV}{=}O}]^{2+} \underset{-\mathrm{H^+},-e^-}{\overset{+\mathrm{H^+},+e^-}{\rightleftharpoons}} [\mathrm{Ru^{III}{-}OH}]^{2+} \underset{-\mathrm{H^+},-e^-}{\overset{+\mathrm{H^+},+e^-}{\rightleftharpoons}} [\mathrm{Ru^{II}{-}OH_2}]^{2+} \qquad (5)$$

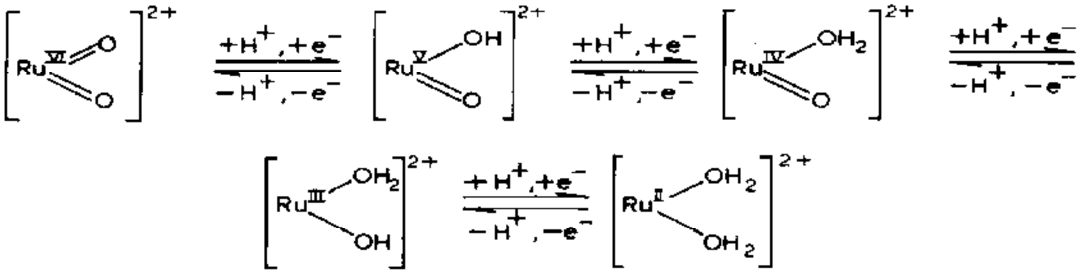

(6)

The fluoride ion is not as effective as the oxide ion in binding high oxidation levels. Thus the existence of RuF_8 is a matter of controversy. However, hexafluoro species occur for all oxidation states in the range +6 to +3, two from the high and two from the intermediate level being covered [13]. The group RuF_6, RuF_6^-, RuF_6^{2-} and RuF_6^{3-} constitutes a potentially interesting and partly explored redox series [34].

(iii) Low states

Among low oxidation states the zero level occurs quite commonly in combination with strong π-acceptor ligands: carbon monoxide, tertiary phosphines and unsaturated organic compounds. The −2 state is very rare and occurs in species such as $Ru(CO)_4^{2-}$ and $Ru(PF_3)_4^{2-}$. The monovalent state is known in dimeric or polymeric metal–metal-bonded species; carbon monoxide is almost invariably present as one of the ligands [13].

(iv) Intermediate states

The intermediate oxidation states are the ones where most of the action lies. These are coordinated with a wide variety of ligands: X–, N–, O–, S–, P–, As– etc. donors (X = halogen). Their ligand and geometric requirements being compatible with one another, these display important interstate phenomena. Two related types will be noted. Firstly, mononuclear species often exhibit facile and reversible redox connectivity (eqn. (7)) (electrons and charges are not shown):

$$\mathrm{Ru^{IV}L} \rightleftharpoons \mathrm{Ru^{III}L} \rightleftharpoons \mathrm{Ru^{II}L} \qquad (7)$$

It may not be possible to isolate all three species in a pure state in every case, but their formation in solution can be frequently demonstrated. Secondly, and as a corollary to the processes of eqn. (7), mixed-valence polynuclear species are formed quite readily. This aspect of ruthenium chemistry has been the centre of great interest. The five possible state combinations of a dimer are shown in eqn. (8):

$$\mathrm{Ru^{IV}LRu^{IV}} \rightleftharpoons \mathrm{Ru^{IV}LRu^{III}} \rightleftharpoons \mathrm{Ru^{III}LRu^{III}} \rightleftharpoons \mathrm{Ru^{III}LRu^{II}} \rightleftharpoons \mathrm{Ru^{II}LRu^{II}} \qquad (8)$$

The redox equilibration in eqn. (8) is hypothetical but is entirely feasible in principle. Both mixed-valence types in eqn. (8) are well documented in ruthenium chemistry.

(v) Backbonding in ruthenium(II)

In several ways, ruthenium(II) occupies a unique position among bivalent metal ions [35]. The antibonding $4d\sigma$ (e_g in O_h symmetry) orbitals are empty while the $4d\pi$ (t_{2g}) orbitals are fully occupied. The extension of the latter orbitals into space is optimal for forming strong bonds with empty π orbitals of an associated ligand. Backbonding of this type is a dominant feature in the chemistry of ruthenium(II). Remarkable manifestations of such bonding can be seen in the lengthening of (1) Ru–L distances in going from the bivalent to the trivalent metal [36,37] and (2) certain bond distances (compared with distances in the free ligand) within the π-acceptor ligand in ruthenium(II) species [38,39]. The effect of backbonding on chemical, photochemical and electrochemical reactivity of ruthenium(II) complexes is very profound.

D. OXIDATION LEVELS OF FREE AND RUTHENIUM-BOUND LIGANDS

(i) General considerations

Electrochemically accessible electron transfer can occur at a coordinated ligand site when the site possesses one or more low lying unoccupied orbitals and/or one or more not-too-stable occupied orbitals. The former can act as reduction orbitals which afford lower oxidation states ($L^{-\cdot}$, L^{2-} etc.) by accepting electrons and the latter as oxidation orbitals which furnish higher oxidation states ($L^{+\cdot}$, L^{2+} etc.) by ionization.

From the above-mentioned energy criteria, it is clear that unsaturated ligands with a well-defined π-orbital system should be good candidates for display of variable oxidation levels. For effective σ-linking to the metal ion, such ligands should also have sites (such as N and/or O) which form part of the π system but also have lone pairs. Most ruthenium complexes displaying variable ligand oxidation levels abide by these rules. The systems covered in this review are **4**–**7**. The chelate rings contain a part or the whole of the ligand π-frame. The Ru–N and Ru–O bonds are predominantly σ in nature, with possible π components (e.g. RuL π backbonding in the case of ruthenium(II) species).

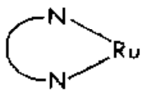

2,2′-bipyridine,
related heterocycles,
2-(arylazo)pyridines,
quinone diimines

4

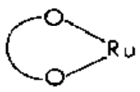

quinones

5

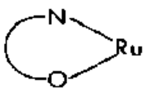

flavins

6

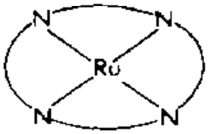

porphyrins,
phthalocyanines

7

When the redox orbitals are essentially ligand in character, a given ligand should display the same pattern of electron transfer in free and coordinated states. However, the E_{T}° values are expected to be substantially different in the two cases. Thus lower ligand oxidation states are expected to be stabilized (higher E_{T}° values) when the ligand becomes bound to a metal cation. In most cases this is found to be true in practice.

(ii) 2,2′-Bipyridine

(a) Accessible oxidation states

Ruthenium complexes of 2,2′-bipyridine (bpy, **8**), its substituted deriva-

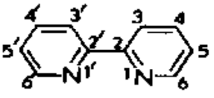

(bpy)

8

tives and analogues (see Section D(iii)) have been of great interest for the past 15 years or so primarily because of their fascinating redox, photophysical and photochemical properties [13,40,41], and therefore only the salient features will be considered in this review. The prototype bpy complex is the red tris chelate cation $[\mathrm{Ru^{II}(bpy)_3}]^{2+}$ reported by Burstell in 1936. Cyclic voltammetry in MeCN [42] and polarography in dmf [43] first revealed that this complex is but one member of a relatively extensive redox series involving metal oxidation and ligand reduction. These results were further augmented in later studies [44,45] and voltammetric experiments in liquid sulphur dioxide, which has a wide voltage window at positive potentials, demonstrated that the redox series is extendable up to one stage of ligand oxidation [46,47]. In summary, the following oxidation states of ruthenium-coordinated bpy are electrochemically accessible: bpy^{2-}, $\mathrm{bpy}^{-\cdot}$, bpy and $\mathrm{bpy}^{+\cdot}$. Among these, the two middle members are most important in terms of tractable chemistry.

(b) Redox series of $[Ru(bpy)_3]^z$ (z = 3, 2, 1, 0, −1): one-electron reduction of each bpy

In MeCN or dmf solution at room temperature, four successive reversible (ΔE_p, 60–70 mV) one-electron cyclic voltammetric responses are observed for $[\mathrm{Ru(bpy)_3}]^{2+}$ at a platinum electrode [42–44,48–51]. The E°_{298} values in MeCN are 1.32, −1.30, −1.49 and −1.73 V [42] and in dmf are 1.24, −1.27, −1.46 and −1.70 V [44]. The response at positive potentials corresponds to the metal oxidation couple $[\mathrm{Ru^{III}(bpy)_3}]^{3+}/[\mathrm{Ru^{II}(bpy)_3}]^{2+}$. The oxidized cation is green in colour and the salts are well characterized. The three couples at negative potentials represent successive reductions of coordinated bpy one after another as shown in eqn. (9):

$$\begin{tikzcd}[\mathrm{Ru(bpy)_3}]^{2+} \arrow[r, shift left, "+e^-"] & {[\mathrm{Ru(bpy)_2(bpy^{-\cdot})}]^{+}} \arrow[l, shift left, "-e^-"] \arrow[r, shift left, "+e^-"] & {[\mathrm{Ru(bpy)(bpy^{-\cdot})_2}]^{0}} \arrow[l, shift left, "-e^-"] \arrow[d, shift left, "+e^-"] \\ & & {[\mathrm{Ru(bpy^{-\cdot})_3}]^{-}} \arrow[u, shift left, "-e^-"]\end{tikzcd} \qquad (9)$$

The redox orbital accommodating the odd electron is the lowest unoccupied

π^* (ψ) molecular orbital [52] of bpy. The four species in eqn. (9) differ in net charge, and in subsequent discussions they will be simply identified as $[Ru(bpy)_3]^z$ where z is the charge as applicable. Free bpy also undergoes electrochemical reduction but only below -2 V, and the process is irreversible at room temperature [42,44,48]. The coordinated ligand is reduced at a much less negative potential, as expected.

As a corollary to the above discussion, species of type $[Ru(bpy)_2L]^z$, where L is electroinactive and occupies two coordination sites, would be expected to display a pair of one-electron reduction waves due to the two bpy ligands. Many examples of this have been documented [53–55]. For $[Ru(bpy)_2(py)_2]^{2+}$, the reduction potentials in MeCN are -1.32 and -1.56 V.

(c) Spatial isolation of redox orbitals

Compelling evidence is now available to show that each added electron is largely localized (C_{2v} symmetry for the reduced complex) in a single chelate ring, as already implied in eqn. (9), and is not delocalized (D_3 symmetry) over all three rings. In other words, the three redox orbitals of the three chelate rings are isolated from one another spatially [44,56–58]. For example, $S = 1/2$ EPR spectra ($g \approx 2$) are observed for all the reduced species, $[Ru(bpy)_3]^z$ ($z = +1, 0, -1$). Spectral band shapes further suggest the presence of a pseudo spin-rotational electron-hopping process in the case of $z = +1$ and 0. The $z = +1$ case is depicted in structure **9**. The activation barrier to this hopping process is about 1000 cm^{-1} [56].

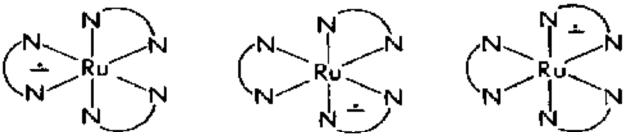

9

(d) Complete redox series: two one-electron reductions of each bpy

Attention has been directed towards realizing species which are more reduced than $[Ru(bpy)_3]^-$. Attempted reduction in MeCN or dmf at room temperature beyond the $z = -1$ stage affords cyclic voltammetric responses (below -2 V) due to free bpy. The latter arises from rapid decomposition following reduction to $z < -1$ [42,50]. However, in very dry dmf at 219 K the cathodic potential window becomes substantially extended and six successive reversible one-electron reduction processes are then observable (Fig. 1). These correspond to the formation of one, two and three coordinated bpy^{2-} moieties in the last three stages of reduction [45]. By utilizing

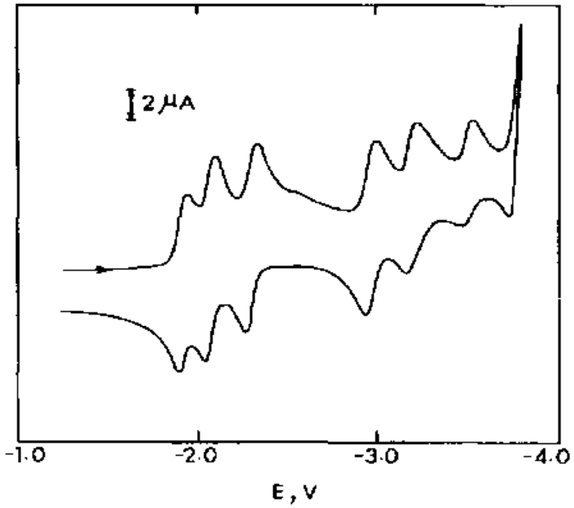

Fig. 1. Cyclic voltammogram (dmf, teah/Pt) of $[Ru(bpy)_3]^{2+}$ at 219 K (adapted from ref. 45).

ligands bearing electron-withdrawing substituents which shift the potentials to higher values, it is possible to observe all six reductions at room temperature in dmf [44]. A representative example is schematically displayed in Fig. 2. Interestingly, the potential gap between the third and fourth reduction steps is substantially larger than that between any other neighbouring pair of couples. In the fourth step an electron is added for the first time to a bpy^- ligand.

(iii) bpy-Like ligands

(a) Tris(bidentate) and bis(tridentate) species

A variety of bpy-like heterocycles and their ruthenium(II) complexes have been subjected to voltammetric examination. Selected examples of such ligands are **10**–**19** [42,49,59–65]. Reduction potential data are shown in

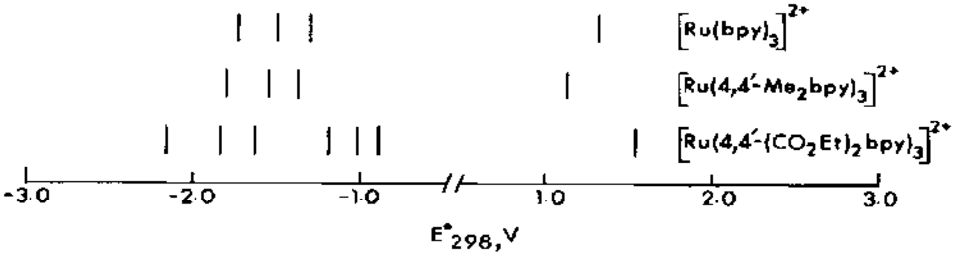

Fig. 2. Formal potentials (dmf, tbah/Pt) of tris complexes of bpy and some substituted derivatives.

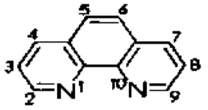

1,10- phenanthroline
(phen)

10

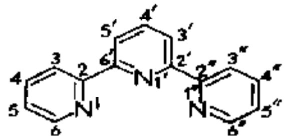

2,2',2"- terpyridine
(terpy)

11

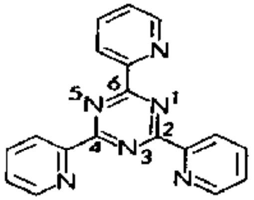

2,4,6 - tripyridyl-s-triazine

(tptz)

12

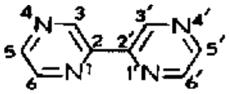

2,2'- bipyrazine
(bpyz)

13

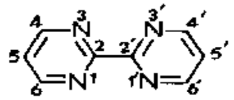

2,2'- bipyrimidine
(bpym)

14

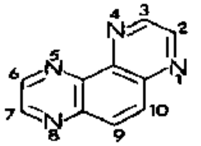

1,4,5,8 - tetraaza-
phenanthrene
(tapt)

15

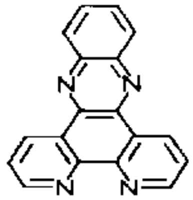

dipyrido [3,2-a; 2',3'-c]-
phenazine
(dph)

16

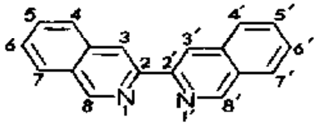

2,2'-biisoquinoline

(i-biq)

17

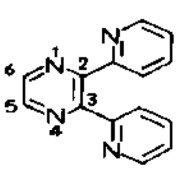

2,3 - bis(2-pyridyl)
pyrazine
(bpp)

18

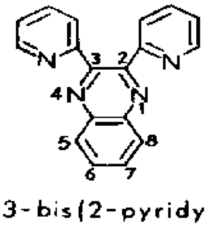

2,3 - bis(2-pyridyl)-
quinoxaline
(bpq)

19

TABLE 3

The bpy and bpy-like systems

Species	Conditions	E°_{298} (V)						Ref.
		Free ligand	Complex					
			Metal	Ligand				
			3+/2+	2+/1+	1+/0	0/1−	1−/2−	
bpy	MeCN, tbab/Pt	−2.13						42
	MeCN, teap/Pt	−2.21, −2.46						48
$[Ru(bpy)_3]^{2+}$	MeCN, tbab/Pt		1.32	−1.30	−1.49	−1.73		42
	dmf, tbap/Hg			−1.25	−1.43	−1.68		43
phen	MeCN, tbab/Pt	−2.10						42
$[Ru(phen)_3]^{2+}$	MeCN, tbab/Pt		1.40	−1.41	−1.54	−1.84		42
terpy	MeCN, tbab/Pt	−2.15						42
$[Ru(terpy)_2]^{2+}$	MeCN, tbab/Pt		1.25	−1.40	−1.65			42
	dmf, tbab/Pt		1.26	−1.26	−1.51	−1.94	−2.34	56
tptz	MeCN, tbab/Pt	−1.56, −2.05						42
$[Ru(tptz)_2]^{3+}$	MeCN, tbab/Pt		1.48	−0.80	−0.96	−1.62	−1.87	42
bpym	MeCN, teap/Pt	−1.99						49
$[Ru(bpym)_3]^{2+}$	MeCN, teap/Pt		1.69	−0.91	−1.08	−1.28		49
bpyz	MeCN, teah/Pt	−1.76						59
$[Ru(bpyz)_3]^{2+}$	MeCN, teap/Pt		1.98	−0.68	−0.87	−1.14		49
	MeCN, teah/Pt		1.86	−0.80	−0.98	−1.24		59
tapt	dmf, tbai/Hg	−1.50, −2.10						61
$[Ru(tapt)_3]^{2+}$	dmf, tbai/Hg			−0.76	−0.86	−1.05		61
	MeCN, tbai/Pt		1.93	−0.76	−0.89	−1.15		61
dph	MeCN, tbab/Pt	−1.29						62
$[Ru(dph)_3]^{2+}$	MeCN, tbab/Pt		1.37	−1.00	−1.08	−1.29		62
$[Ru(i\text{-biq})_3]^{2+}$	MeCN, tbap/Pt		1.00	−1.63	−1.88			63
$[Ru(bpp)_3]^{2+}$	MeCN, tbah/Pt		1.68	−0.95	−1.12	−1.39		64
bpq	MeCN, teap/Pt	−1.56						65
$[Ru(bpq)_3]^{2+}$	MeCN, teap/Pt		1.70	−0.60	−0.78	−1.04		65

Table 3. The observed redox patterns are generally analogous to those of bpy and $[\mathrm{Ru(bpy)_3}]^{2+}$. The salient features are as follows. The complexes give rise to a ruthenium(III)/ruthenium(II) couple and a ligand reduction series. One-electron reduction of each coordinated ligand is facile. Free-ligand reduction occurs at more negative (by ca. 1 V) potential than bound-ligand reduction. In fact, the plot of reduction potentials of free ligands vs. those of bound ligands is linear with unit slope [65]. Redox π^* orbitals of different ligands within the same molecule are spatially isolated.

(b) Mixed complexes

In mixed-ligand complexes the first reduction may be expected to involve the ligand having the most stable lowest unoccupied molecular orbital (LUMO) [49]. Selected formal potentials are given in Table 4. Mixed bpy–bpyz complexes are good examples. The bpyz LUMO lies lower than the bpy LUMO [59]. The three successive reductions of $[\mathrm{Ru(bpy)_2(bpyz)}]^{2+}$ are assignable to the couples in eqn. (10):

$$[\mathrm{Ru(bpy)_2(bpyz)}]^{2+} \underset{-e^-}{\overset{+e^-}{\rightleftharpoons}} [\mathrm{Ru(bpy)_2(bpyz^{-\bullet})}]^{+} \underset{-e^-}{\overset{+e^-}{\rightleftharpoons}} [\mathrm{Ru(bpy)(bpy^{-\bullet})(bpyz^{-\bullet})}]^{0} \underset{-e^-}{\overset{+e^-}{\rightleftharpoons}} [\mathrm{Ru(bpy^{-\bullet})(bpy^{-\bullet})(bpyz^{-\bullet})}]^{-} \qquad (10)$$

These have E°_{298} values of -0.91 V, -1.45 V and -1.68 V respectively in MeCN, teap/Pt. The same effect is observed in the voltammogram in Fig. 3 where the reductions of bound bpyz and bpy lie near 1 V and 1.5 V respectively [49].

TABLE 4

Mixed-tris complexes

Species	Conditions	E°_{298} (V)				Ref.
		Metal	Ligand			
		3+/2+	2+/1+	1+/0	0/1−	
$[\mathrm{Ru(bpyz)_2(bpy)}]^{2+}$	MeCN, teap/Pt	1.72	−0.79	−1.02	−1.58	49
$[\mathrm{Ru(bpyz)(bpy)_2}]^{2+}$	MeCN, teap/Pt	1.49	−0.91	−1.45	−1.68	49
$[\mathrm{Ru(bpym)_2(bpy)}]^{2+}$	MeCN, teap/Pt	1.55	−0.95	−1.13		49
$[\mathrm{Ru(bpym)(bpy)_2}]^{2+}$	MeCN, teap/Pt	1.40	−1.02	−1.45		49
$[\mathrm{Ru(\mathit{i}\text{-}biq)_2(bpy)}]^{2+}$	MeCN, tbap/Pt	1.05	−1.54	−1.76	−1.86	63
$[\mathrm{Ru(\mathit{i}\text{-}biq)(bpy)_2}]^{2+}$	MeCN, tbap/Pt	1.10	−1.50	−1.69	−1.84	63
$[\mathrm{Ru(bpp)(bpy)_2}]^{2+}$	MeCN, tbah/Pt	1.31	−1.06	−1.50		64
$[\mathrm{Ru(bpq)_2(bpy)}]^{2+}$	MeCN, teap/Pt	1.53	−0.66	−0.89	−1.58	65
$[\mathrm{Ru(bpq)(bpy)_2}]^{2+}$	MeCN, teap/Pt	1.39	−0.78	−1.45		65

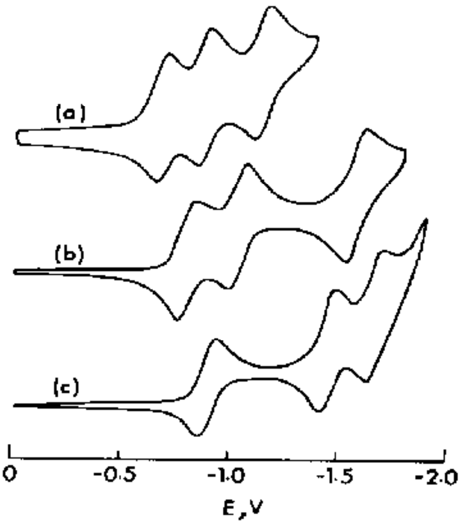

Fig. 3. Cyclic voltammograms (MeCN, teap/Pt) of (a) $[Ru(bpyz)_3]^{2+}$, (b) $[Ru(bpyz)_2(bpy)]^{2+}$ and (c) $[Ru(bpyz)(bpy)_2]^{2+}$ at 298 K (adapted from ref. 49).

A decrease in the σ-donor capacity of coordinated ligands increases both the ruthenium(III)/ruthenium(II) and the first bound-ligand reduction potentials, the effect being more pronounced in the former. The two potentials correlate linearly. A decrease in ligand σ-donor ability can be achieved by placing electron-withdrawing substituents on a given ligand type [44] or by replacement of one ligand by another [49,65]. The latter situation is represented by the two series $[Ru(bpyz)_3]^{2+}$, $[Ru(bpyz)_2(bpy)]^{2+}$, $[Ru(bpyz)(bpy)_2]^{2+}$ and $[Ru(bpym)_3]^{2+}$, $[Ru(bpym)_2(bpy)]^{2+}$, $[Ru(bpym)(bpy)_2]^{2+}$ [49], and the relevant formal potential data are collected in Table 4. For the three ligands concerned, σ-donor strength decreases in the order bpy > bpym > bpyz. The observed variation in formal potentials is rationalized as follows. A decrease in σ-donor capacity leads to an increase in the effective charge on ruthenium, and this in turn stabilizes metal $d\pi$-orbitals directly and ligand π^*-orbitals indirectly through charge interactions. Subsequent $d\pi-\pi^*$ backbonding further stabilizes the metal $d\pi$-orbitals but destabilizes ligand π^*-orbitals [49]. The net effect is thus more pronounced in the ruthenium(III)/ruthenium(II) couple than in the bound-ligand reduction. The slope of the linear plot of the two potentials is therefore greater than unity (Fig. 4).

(c) *Substituted species with additional redox orbitals*

We now cite a case where substitution at bpy is such as to add new redox orbitals. In complexes of 1,10-phenanthroline-5,6-dione (ptd) (chelate ring **20**) the ligand is a quinone and can in principle accept two electrons

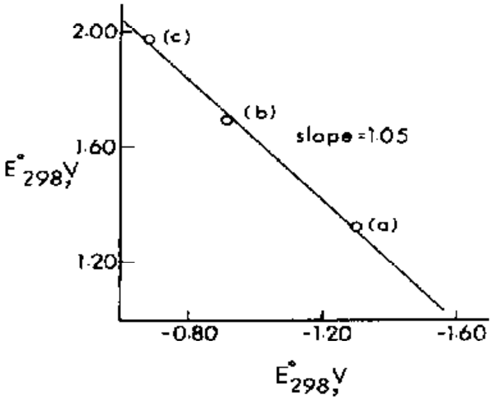

Fig. 4. Correlation between the ruthenium(III)/ruthenium(II) (y axis) and first bound-ligand (x axis) reduction potentials (MeCN, teap/Pt) of (a) $[Ru(bpy)_3]^{2+}$, (b) $[Ru(bpym)_3]^{2+}$ and (c) $[Ru(bpyz)_3]^{2+}$.

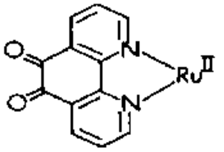

20

successively, forming a semiquinone and quinone respectively (see Section D(vi)). In MeCN solution the complex $[Ru^{II}(bpy)_2(ptd)]^{2+}$ exhibits five one-electron reversible cyclic voltammetric waves which have been assigned as follows: 1.35 V, ruthenium(III)/ruthenium(II); −0.07 and −0.77 V, successive reductions of ptd; −1.39 and −1.59 V, successive reductions of the two bpy ligands. Surprisingly, $[Ru^{II}(ptd)_3]^{2+}$ displays only two (E°_{298}, −0.13 and −0.86 V) reduction waves; apparently all three ptd ligands are electroactive at the same potential [66].

Another possible case is represented by complexes of the bipyridyl pyridazine ligand (dp) which binds to ruthenium as in **21**. The complexes

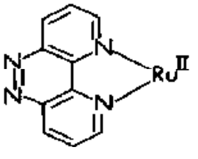

21

$[Ru(bpy)_{3-n}(dp)]^{2+}$ ($n = 1, 2, 3$) display the first one-electron reduction at ca. −0.7 V. The redox orbital has been assigned to be bpy like, with the exception that it is symmetric (χ), unlike in the case of bpy (ψ, see below) [67]. These authors have, however, ignored the possibility that the reduction may actually involve the azo function (see Section D(iv)) rather than the bpy fragment.

(iv) Azo donors

(a) Free ligands

Sadler and Bard have reported an electrochemical study of a series of aromatic azo compounds in dmf [68]. The redox orbital is the π^*(azo) orbital. Reduction occurs in two successive one-electron steps (eqns. (11) and (12)):

$$[-\mathrm{N}{=}\mathrm{N}-] + e^- \rightleftharpoons [-\mathrm{N}\overset{\cdots}{-}\mathrm{N}-]^- \tag{11}$$

$$[-\mathrm{N}\overset{\cdots}{-}\mathrm{N}-]^- + e^- \rightleftharpoons [-\mathrm{N}-\mathrm{N}-]^{2-} \tag{12}$$

The product of the first electron transfer is a relatively stable anion radical, but the dianion formed in the second step undergoes facile secondary chemical transformations. For azobenzene, the E°_{298} values of the couples (11) and (12) are -1.36 V and -2.03 V respectively. The azo function can also undergo an irreversible one-electron oxidation [69,70], but in this review we shall be concerned only with the three oxidation levels implicated in eqns. (11) and (12).

Of particular interest in the context of ruthenium complexes is the behaviour of 2-(arylazo)pyridine (aap) **22**. In MeCN solvent, the free pap ligand displays two quasi-reversible one-electron cyclic voltammetric responses with peak-to-peak separations in the range 120–150 mV, corresponding to the couples in eqns. (13) and (14):

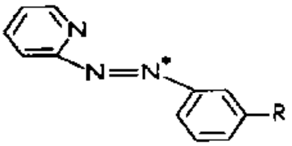

(aap)
R=H ; pap
R=Me; tap
22

$$\mathrm{pap} + e^- \rightleftharpoons \mathrm{pap}^{-\cdot} \tag{13}$$

$$\mathrm{pap}^{-\cdot} + e^- \rightleftharpoons \mathrm{pap}^{2-} \tag{14}$$

The formal potentials of these couples are respectively -1.31 V and -1.57 V. As for azobenzene, the redox orbital is primarily π^*(azo) in character and the couples (13) and (14) essentially correspond to the processes in eqn. (11) and eqn. (12) respectively [71].

(b) Complete redox series in [Ru(aap)$_3$]$^{2+}$

Ruthenium complexes of substituted azobenzene [72,73] and other azo ligands [74–76] have been subjected to electrochemical examination in several instances, but the primary emphasis in these studies has been on metal redox. However, both metal and ligand oxidation levels have received attention for complexes of aap [71,77–85]. With respect to ruthenium(II), this ligand system is a better π-acceptor (the acceptor orbital is π*(azo)) than bpy and bpy-like ligands. Consequently, Ru^{II}aap backbonding is stronger than Ru^{II}bpy backbonding. Significantly, the Ru–N(azo) distance is shorter than the Ru–N(py) distance [37,38].

The tris complexes [Ru(aap)$_3$]$^{2+}$ have meridional geometry (**23**) and

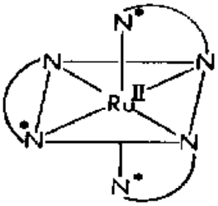

23

display the [Ru^{III}(aap)$_3$]$^{3+}$/[Ru^{II}(aap)$_3$]$^{2+}$ couple above 2 V. Six successive one-electron reductions can occur in principle owing to the three azo groups. In anhydrous MeCN, all the reductions can indeed be observed in differential pulse voltammetric experiments using a mercury electrode. Selected results are shown in Table 5 and Fig. 5. As expected, the first reduction

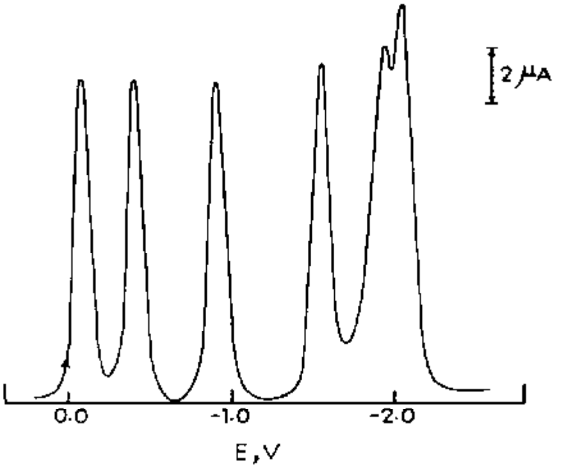

Fig. 5. Differential pulse voltammogram (MeCN, teap/Hg) of *mer*-[Ru(tap)$_2$(pap)](ClO$_4$)$_2$·H$_2$O at 298 K (adapted from ref. 71).

TABLE 5

Complexes of aap

Species[a]	E°_{298} (V)	$-E^{\circ}_{298}$ (V)						Ref.
	Metal[b]	Ligand[c]						
	3+/2+	2+/1+	1+/0	0/1−	1−/2−	2−/3−	3−/4−	
mer-$[Ru(pap)_3](ClO_4)_2 \cdot H_2O$	2.10	0.13	0.45	0.94	1.59	1.92	2.06	71
mer-$[Ru(tap)(pap)_2](ClO_4)_2 \cdot H_2O$	2.14	0.11	0.43	0.91	1.57	1.92	2.04	71
mer-$[Ru(tap)_2(pap)](ClO_4)_2 \cdot H_2O$	2.19	0.08	0.41	0.91	1.57	1.93	2.03	71
mer-$[Ru(tap)_3](ClO_4)_2 \cdot H_2O$	2.23	0.10	0.43	0.93	1.59	1.89	1.95	71
tc-$[Ru(en)(tap)_2](ClO_4)_2 \cdot H_2O$	1.69	0.32	0.93	1.60	1.80			71
tc-$[Ru(bpy)(pap)_2](ClO_4)_2 \cdot H_2O$	1.88	0.21	0.72	1.47	1.75	2.06	2.44	71
$[Ru(bpy)_2(pap)](ClO_4)_2 \cdot H_2O$	1.60	0.52	1.26	1.81	2.15	2.53		71
tc-$[Ru(acac)(tap)_2]ClO_4 \cdot H_2O$	1.34	0.41	0.98	1.90				71
tc-$[Ru(Ph_2P(CH_2)_2PPh_2)(tap)_2](ClO_4)_2 \cdot H_2O$	2.24	0.16[d]	0.57[d]	1.36[d]				78

[a] Abbreviations: en, ethylenediamine; acac, acetylacetonate.

[b] MeCN, teap/Pt.

[c] MeCN, teap/Hg, unless otherwise stated.

[d] MeCN, teap/Pt.

potential displays a substantial positive shift from the corresponding free ligand value.

Both aap and bpy have one electrochemically accessible redox orbital. However, the π^*(azo) orbital of the former is substantially more stable than the $\pi^*(\psi)$ orbital of the latter. The reduction potentials of the former are systematically higher (by ca. 1 V) than the corresponding potentials of the latter, both in the free and in the complexed states. Indeed, the reduction potentials of the aap system are higher than those of all bpy-like ligands. The observation of six reductions in $[Ru(bpy)_3]^{2+}$ requires special experimental conditions so as to make the required highly negative potentials accessible (see Section D(ii)(d)) [45]. The electronic structures of the reduced derivatives of $[Ru(aap)_3]^{2+}$ have not been carefully investigated so far, but there are strong indications that the three ligand redox orbitals are spatially isolated (eqn. (15)) as in the case of bpy [71,85]:

$$\begin{tikzcd}
[Ru(aap)_3]^{2+} \arrow[r, shift left, "+e^-"] & [Ru(aap)_2(aap^{-\cdot})]^{+} \arrow[l, shift left, "-e^-"] \arrow[r, shift left, "+e^-"] & [Ru(aap)(aap^{-\cdot})_2]^{0} \arrow[l, shift left, "-e^-"] \arrow[d, shift right, "+e^-"'] \\
 & & [Ru(aap^{-\cdot})_3]^{-} \text{ etc.} \arrow[u, shift right, "-e^-"']
\end{tikzcd}$$

(15)

Lastly, it is noted that the aap ligand contains the azo-imine function –N=N–C=N– which is isoelectronic with the diimine function –N=C–C=N– present in bpy. This analogy is, however, of only formal value and has little practical utility since the aap LUMO is essentially localized in the azo fragment.

(c) Mixed species

Complexes of type $[Ru^{II}(aap)_2L]^z$ where L is a bidentate neutral or

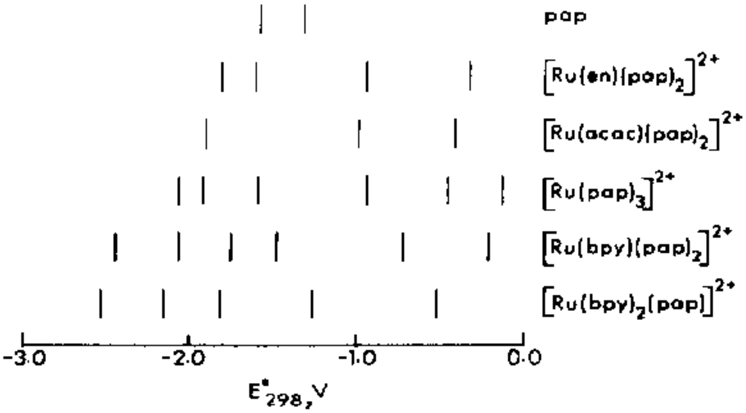

Fig. 6. Ligand reduction potentials (MeCN, teap/Hg) of free aap, tris and mixed-tris complexes (adapted from ref. 71).

anionic ligand have been reported [71,78,80,81,83–85]. When L is electroinactive, all or most of the four expected azo reductions are observable. The complexes where L = en, acac, $Ph_2P(CH_2)_2PPh_2$ are listed in Table 5. $[Ru(aap)_2(bpy)]^{2+}$ and $[Ru(aap)(bpy)_2]^{2+}$ are interesting in that both types of ligand are electroactive. In the former, all the six expected reductions are observed, but in the latter the last reduction is inaccessible (Table 5). It has been proposed that in the bpy–aap mixed complexes, the aap ligand(s) is(are) completely reduced (aap → $aap^{-\cdot}$ → aap^{2-}) before bpy reduction occurs [71]. The successive reduction potentials of a group of complexes are graphically presented in Fig. 6.

(d) Correlation of reduction potential with charge transfer

Normally, ruthenium(II) complexes of unsaturated ligands displaying the electrochemical responses shown in eqns. (16) and (17)

$$[Ru^{III}L]^+ + e^- \rightleftharpoons [Ru^{II}L] \tag{16}$$

$$[Ru^{II}L] + e^- \rightleftharpoons [Ru^{II}L^{-\cdot}] \tag{17}$$

also show allowed electronic transition(s) in the visible region owing to metal-to-ligand charge transfer (MLCT) of the type $t_2 \rightarrow \pi^*$. In simple terms the excitation process which involves intramolecular redox can be represented as

$$[Ru^{II}L] \xrightarrow{\text{MLCT}} [RuL]^* \equiv [Ru^{III}L^{-\cdot}] \tag{18}$$

The energy ν_{CT} of the lowest MLCT transition is expected to be related in some simple manner with the reduction potentials of the couples in eqns. (16) and (19):

$$[Ru^{III}L]^+ + e^- \rightleftharpoons [Ru^{III}L^{-\cdot}] \tag{19}$$

However, the last couple is not experimentally observable, as metal reduction (eqn. (16)) precedes ligand reduction which is observed only in the form of eqn. (17). The redeeming practical feature is that a meaningful correlation is still possible with the observable couples (eqns. (16) and (17)). The potential difference defined in eqn. (20) as

$$\Delta E° = E°(16) - E°(17) \tag{20}$$

varies linearly with ν_{CT}. This was first noted in a sizeable group of complexes of $[Ru(aap)_2]^{2+}$ with various coligands [71]. Data are collected in Table 6. The ligands used include triazene 1-oxides (Rto, **24**), hydroxamates (RR′hya, **25a**) and hydroximates (R′hyi, **25b**).

TABLE 6

Spectroelectrochemical data of some aap complexes

Species [a]	$E^{\circ}_{298}(16)$ [b] (V) Metal	$E^{\circ}_{298}(17)$ [b] (V) Ligand	ΔE° (V)	ν_{CT} (cm^{-1})		Ref.
				Obs. [c]	Calc. [d]	
tc-$[Ru(Ph_2P(CH_2)_2PPh_2)(tap)_2](ClO_4)_2 \cdot H_2O$	2.24	−0.16	2.40	21010	21280	78
tc-$[Ru(PPhMe_2)_2(tap)_2](ClO_4)_2 \cdot H_2O$	2.04	−0.32	2.36	20410	21010	78
tc-$[Ru(Ph_2P(CH_2)_3PPh_2)(pap)_2](ClO_4)_2 \cdot H_2O$	2.08	−0.17	2.25	20490	20280	78
tc-$[RuCl(PPh_2Me)(tap)_2]ClO_4 \cdot H_2O$	1.55	−0.51	2.06	18730	19030	78
tc-$[RuCl(PPhMe_2)(pap)_2]ClO_4 \cdot H_2O$	1.54	−0.50	2.04	18660	18890	78
tc-$[RuCl(PPh_2Me)(pap)_2]ClO_4 \cdot H_2O$	1.55	−0.46	2.01	18730	18700	78
tc-$[RuCl(P(p\text{-tol})_3)(pap)_2]ClO_4 \cdot H_2O$	1.50	−0.43	1.93	18660	18170	78
tc-$[RuCl(PPh_3)(pap)_2]ClO_4 \cdot H_2O$	1.50	−0.42	1.92	18660	18100	78
tc-$[RuBr(PPh_2Me)(pap)_2]ClO_4 \cdot H_2O$	1.42	−0.46	1.88	18870	17840	78
tc-$[RuCl(PPh_3)(tap)_2]ClO_4 \cdot H_2O$	1.45	−0.41	1.86	18660	17700	78
mer-$[Ru(pap)(tap)_2](ClO_4)_2 \cdot H_2O$	2.23	−0.08	2.31	20330	20680	71
mer-$[Ru(tap)_3](ClO_4)_2 \cdot H_2O$	2.19	−0.10	2.29	20240	20550	71
mer-$[Ru(tap)(pap)_2](ClO_4)_2 \cdot H_2O$	2.14	−0.11	2.25	20330	20280	71
mer-$[Ru(pap)_3](ClO_4)_2 \cdot H_2O$	2.10	−0.13	2.23	20330	20150	71
$[Ru(btz)(pap)_2](ClO_4)_2$	1.80 [e]	−0.43 [e]	2.23	19420	20150	83
cc-$[Ru(bpy)(tap)_2](ClO_4)_2 \cdot H_2O$	1.92	−0.23	2.15	19610	19620	– [f]
$[Ru(bpy)_2(pap)](ClO_4)_2 \cdot H_2O$	1.60	−0.52	2.12	20240	19420	71
$[Ru(bpy)_2(tap)](ClO_4)_2 \cdot H_2O$	1.60	−0.52	2.12	20240	19420	71
tc-$[Ru(tap)_2(bpy)](ClO_4)_2 \cdot H_2O$	1.89	−0.21	2.11	19530	19360	71
tc-$[Ru(pap)_2(bpy)](ClO_4)_2 \cdot H_2O$	1.88	−0.21	2.09	19460	19230	71
tc-$[Ru(en)(tap)_2](ClO_4)_2 \cdot H_2O$	1.69	−0.32	2.01	18590	18700	71
tc-$[Ru(acac)(tap)_2]ClO_4 \cdot H_2O$	1.34	−0.41	1.75	17730	16980	71
tc-$[Ru(MeCN)(py)(pap)_2](ClO_4)_2 \cdot H_2O$	1.88	−0.32	2.20	19610	19950	80
tc-$[Ru(OH_2)(pic)(pap)_2](ClO_4)_2 \cdot H_2O$	1.88	−0.28	2.16	18870	19690	80
tc-$[Ru(OH)(OH_2)(pap)_2]ClO_4 \cdot H_2O$	1.18	−0.58	1.76	18180	17040	80
cc-$[RuCl_2(tap)_2]$	1.18	−0.55	1.73	17610	16840	– [f]
cc-$[RuCl_2(pap)_2]$	1.16	−0.53	1.69	17540	16580	– [f]

tc-[$RuBr_2(tap)_2$]	1.10	−0.55	1.65	17070	16320	–[f]
tc-[$RuCl_2(tap)_2$]	1.10	−0.49	1.59	17240	15920	–[f]
tc-[$RuCl_2(pap)_2$]	1.05	−0.47	1.52	17240	15460	–[f]
tt-[$RuCl_2(tap)_2$]	0.91	−0.70	1.61	15770	16050	77
tt-[$RuBr_2(tap)_2$]	0.90	−0.69	1.59	15750	15920	77
tt-[$RuI_2(tap)_2$]	0.91	−0.70	1.61	15610	16050	77
tt-[$RuCl_2(pap)_2$]	0.92	−0.69	1.61	15750	16050	77
tt-[$RuBr_2(pap)_2$]	0.95	−0.69	1.64	15750	16250	77
tt-[$RuI_2(pap)_2$]	0.85	−0.70	1.55	15580	15650	77
[$Ru(tu)_2(pap)_2](ClO_4)_2$	1.14[e]	−0.32[e]	1.46	17100	15060	83
tc-[$Ru(MeOto)(pap)_2]ClO_4 \cdot H_2O$	0.71	−0.54	1.25	14080	13670	71
tc-[$Ru(Meto)(pap)_2]ClO_4 \cdot H_2O$	0.78	−0.53	1.31	13740	14070	71
tc-[$Ru(Hto)(pap)_2]ClO_4 \cdot H_2O$	0.82	−0.48	1.30	13700	14000	71
tc-[$Ru(Hto)(tap)_2]ClO_4 \cdot H_2O$	0.81	−0.49	1.30	13370	14000	71
tc-[$Ru(Clto)(pap)_2]ClO_4 \cdot H_2O$	0.84	−0.48	1.32	14010	14130	71
tc-[$Ru(CO_2Etto)(pap)_2]ClO_4 \cdot H_2O$	0.89	−0.42	1.31	13970	14070	71
tc-[$Ru(NO_2to)(pap)_2]ClO_4 \cdot H_2O$	0.93	−0.41	1.34	14080	14270	71
tc-[$Ru(MeMeOhya)(pap)_2]ClO_4 \cdot H_2O$	1.03	−0.44	1.47	15040	15120	81
tc-[$Ru(MeMehya)(pap)_2]ClO_4 \cdot H_2O$	1.05	−0.44	1.49	15150	15260	81
tc-[$Ru(MeHhya)(pap)_2]ClO_4 \cdot H_2O$	1.06	−0.42	1.48	14930	15190	81
tc-[$Ru(MeClhya)(pap)_2]ClO_4 \cdot H_2O$	1.07	−0.42	1.49	15150	15260	81
tc-[$Ru(MeNO_2hya)(pap)_2]ClO_4 \cdot H_2O$	1.10	−0.41	1.51	15040	15390	81
tc-[$Ru(PhMeOhya)(pap)_2]ClO_4 \cdot H_2O$	1.08	−0.42	1.50	15380	15320	81
tc-[$Ru(PhMehya)(pap)_2]ClO_4 \cdot H_2O$	1.10	−0.42	1.52	15150	15460	81
tc-[$Ru(PhHhya)(pap)_2]ClO_4 \cdot H_2O$	1.11	−0.41	1.52	15380	15460	81
tc-[$Ru(PhClhya)(pap)_2]ClO_4 \cdot H_2O$	1.13	−0.41	1.54	15270	15590	81
tc-[$Ru(PhNO_2hya)(pap)_2]ClO_4 \cdot H_2O$	1.17	−0.40	1.57	15380	15790	81
tc-[$Ru(HMeOhya)(pap)_2]ClO_4 \cdot H_2O$	1.05	−0.42	1.47	15270	15120	81
tc-[$Ru(HMehya)(pap)_2]ClO_4 \cdot H_2O$	1.07	−0.42	1.49	15150	15260	81

TABLE 6 (continued)

Species [a]	$E^\circ_{298}(16)$ [b] (V) Metal	$E^\circ_{298}(17)$ [b] (V) Ligand	ΔE° (V)	ν_{CT} (cm^{-1})		Ref.
				Obs. [c]	Calc. [d]	
tc-[Ru(HHhya)(pap)$_2$]ClO$_4$·H$_2$O	1.08	−0.41	1.49	15150	15260	81
tc-[Ru(HClhya)(pap)$_2$]ClO$_4$·H$_2$O	1.10	−0.40	1.50	15150	15320	81
tc-[Ru(HNO$_2$hya)(pap)$_2$]ClO$_4$·H$_2$O	1.14	−0.39	1.53	15040	15520	81
tc-[Ru(MeOhyi)(pap)$_2$]·H$_2$O	0.33	−0.65	0.98	11980	11880	81
tc-[Ru(Hhyi)(pap)$_2$]·H$_2$O	0.38	−0.63	1.01	12050	12080	81
tc-[Ru(Clhyi)(pap)$_2$]·H$_2$O	0.41	−0.63	1.04	12050	12280	81
tc-[Ru(NO$_2$hyi)(pap)$_2$]·H$_2$O	0.48	−0.60	1.08	12120	12550	81

[a] Abbreviations: *p*-tol, *p*-tolyl; btz, 4,4′-bithiazole; en, ethylenediamine; acac, acetylacetonate; pic, *β*-picoline; tu, thiourea; for MeOto, MeMeOhya, MeOhyi etc. see text (structures **24** and **25**).

[b] MeCN, teap/Pt, unless otherwise stated.

[c] In MeCN.

[d] Using eqns. (20) and (21) of text.

[e] MeCN, NaClO$_4$/Pt.

[f] A. Chakravorty and coworkers, unpublished results.

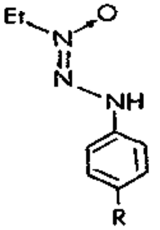

(Rto)

R = MeO, Me, H, Cl, CO_2Et, NO_2

24

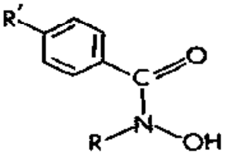

(R R′hyo)

R = Me, Ph, H

R′ = MeO, Me, H, Cl, NO_2

25a

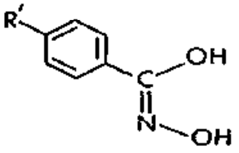

(R′hyi)

R′ = MeO, H, Cl, NO_2

25b

The configuration of the $[Ru(aap)_2]^{2+}$ fragment is *trans–trans (tt)*, **26a**, *trans–cis (tc)*, **26b** or *cis–cis (cc)*, **26c**. The MLCT transition involves

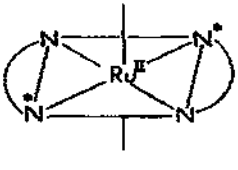

tt

26a

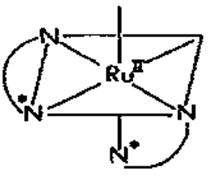

tc

26b

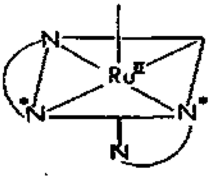

cc

26c

excitation to the azo π^*-orbital [71,85] and the first ligand reduction involves the same orbital as discussed above. The values of $E^\circ(16)$, $E^\circ(17)$, ΔE° (cm^{-1}) are given in Table 6. The least-squares plot (Fig. 7) of ν_{CT} against ΔE° (in volts) corresponds to eqn. (21):

$$\nu_{CT} = 0.82\Delta E^\circ + 0.67 \tag{21}$$

The closeness of this fit can be directly seen in the excellent agreement between experimental transition energies and those calculated with the help of eqn. (21) (Table 6). The ranges of ΔE° (2.3–1.0 V) and ν_{CT} (12 000–21 000 cm^{-1}, 1.5–2.6 eV) covered by this relationship are quite wide.

A similar correlation has been observed for bpy complexes [86–88]. The physical basis of such correlations generally defined by

$$\nu_{CT} = \alpha\Delta E^\circ + \beta \tag{22}$$

has been examined [41,88] and reviewed [41]. Using a thermodynamic cycle, ν_{CT} can be expressed [87] as in eqn. (23):

$$\nu_{CT} = \Delta E^\circ + S + Q \tag{23}$$

where the term S involves the free energies of solvation of the various species ($[Ru^{II}L]$, $[RuL]^*$, $[Ru^{III}L]^+$ and $[Ru^{II}L^{-\cdot}]$) as well as the reorganiza-

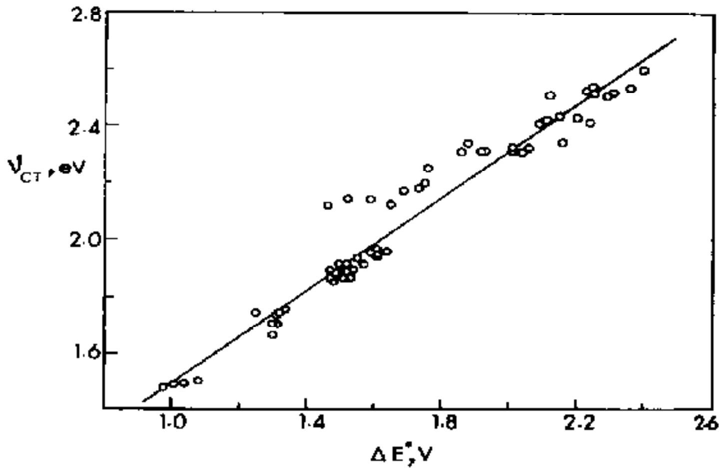

Fig. 7. Least-squares plot of ν_{CT} against ΔE° of some aap complexes (data from Table 6).

tion energies of the excited state. The quantity Q is the energy of the hypothetical electron transfer process in the gas phase.

$$[\mathrm{Ru^{III}L}]^+ + [\mathrm{Ru^{II}L^{-\cdot}}] \longrightarrow [\mathrm{Ru^{II}L}] + [\mathrm{Ru^{III}L^{-\cdot}}]^+ \tag{24}$$

The last equation connects eqns. (17) and (19). In a group of complexes, where only the electroinactive coligand varies, S may be expected to remain more or less constant. However, Q may vary with ΔE° and this may be one of the main reasons for the deviation of the slope α from unity in eqn. (22).

(v) Quinone diimines

(a) Free ligands

The most oxidized form of this class of ligand is illustrated by qd (**27a**). It is related to bpy in that both species contain the diimine fragment –N=C–C=N–. It is also related to quinones (Section D(vi)), the two oxygen atoms of the latter being replaced by two imine functions (=NH). The two other oxidation levels are found in the semiquinone diimine anion radical (sqd, **27b**) and *o*-phenylenediamine dianion (pd, **27c**) [89]. Neither **27a** nor **27b** can be isolated in pure form; only **27c** is isolable in the diprotonated form.

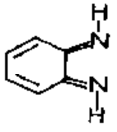

(qd)

27a

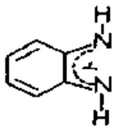

(sqd)

27b

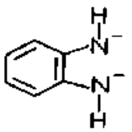

(pd)

27c

(b) $[Ru(qd)_3]^{2+}$

This complex can be prepared by aerobic oxidation of the corresponding pd complex [90]. Assuming that each qd ligand has one electrochemically accessible π^* LUMO, six one-electron reduction waves may be anticipated from this complex. In practice, all these are not observable. MeCN solutions of $[Ru(qd)_3]^{2+}$ display two reversible (E°_{298}, 0.03 and -0.31 V), one quasi-reversible (-1.08 V) and one irreversible (-1.2 V) one-electron reductions [90]. It is very likely that the first two reductions correspond to the successive formation of $[Ru^{II}(qd)_2(sqd)]^+$ and $[Ru^{II}(qd)(sqd)_2]$. The separation between the two E°_{298} values is comparable to that between the first two ligand reduction potentials of $[Ru(bpy)_3]^{2+}$ (Table 3). Attempted oxidation of the metal in $[Ru(qd)_3]^{2+}$ leads to decomposition of the molecule.

(c) Mixed qd–bpy complexes

The species $[Ru(qd)_2(bpy)]^{2+}$, $[Ru(qd)(bpy)_2]^{2+}$ and some other related systems are also described [91]. The structure of $[Ru(qd)(bpy)_2](PF_6)_2$ is accurately known. The Ru–N(qd) distance is shorter than the Ru–N(bpy) distance (2.02(1) Å and 2.08(1) Å respectively). This has been attributed to the π-backbonding order $Ru^{II}_{qd} > Ru^{II}_{bpy}$.

The complex $[Ru(qd)_2(bpy)]^{2+}$ displays the metal oxidation couple (ruthenium(III)/ruthenium(II)) E°_{298}, 1.13 V. Multiple reductions are observed at negative potentials. The first two reduction couples (E°_{298}, -0.48 and -0.93 V) are well formed and are presumably due to successive reductions of the complexed qd to sqd. A comparison of these results with those in Table 3 shows that the reduction $Ru^{II}qd \rightarrow Ru^{II}sqd$ occurs at a much higher potential than $Ru^{II}bpy \rightarrow Ru^{II}bpy^{-\cdot}$. The LUMO of qd lies considerably lower than that of bpy. The higher π backbonding by qd compared with that by bpy (see below) is compatible with this. A similar comparison was made between bpy and aap in Section D(iv). The qd reductions occur at a potential even more positive than those of aap reductions.

Ligand-based reduction has also been observed in the ruthenium-bound *p*-quinone diimine system **28** [92,93].

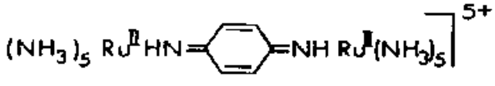

28

(vi) Quinones

(a) Free ligands

The *o*-quinonoid system (**29**) spans three oxidation levels: quinone (Rq, **29a**), semiquinone anion radical (Rsq, **29b**) and hydroquinone or catechol dianion (Rcq, **29c**). Quinones and catechols are known in pure form. Paramagnetic semiquinones are usually generated and studied in solution. These have a characteristic strong EPR signal near $g = 2.00$ [94]. By virtue of their frequent occurrence in the living world, the quinones have received considerable attention from organic chemists and biochemists [95,96].

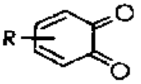
(Rq)
29a

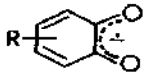
(Rsq)
29b

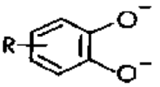
(Rcq)
29c

In aprotic media, the three oxidation levels of **29** are observable voltammetrically (eqn. (25)):

$$\text{Rq} \underset{-e^-}{\overset{+e^-}{\rightleftarrows}} \text{Rsq} \underset{-e^-}{\overset{+e^-}{\rightleftarrows}} \text{Rcq} \tag{25}$$

The formal potentials of the two couples [97] are given in Table 7. Upon protonation, Rsq disproportionates into an equimolecular mixture of Rq and H_2Rcq. When a proton source is present in the solution, the electrochemistry of **29** becomes complex owing to this and other reactions [97].

(b) Complexes: a general principle

The quinonoid system can chelate transition metal ions as a bidentate *O,O*-ligand. Central to the chemistry of such chelates is the question of the

TABLE 7

The *o*-quinonoid systems [a]

Compounds	Conditions	E°_{298} (V)		Ref.
		Rq/Rsq	Rsq/Rcq	
dbcq	MeCN, teap/Pt	−0.51	−1.30	97
Hcq	MeCN, teap/Pt	−0.31	−0.92	97
tccq	MeCN, teap/Pt	0.18	−0.60	97
$[Ru(tccq)(CO)_2(PPh_3)_2]$ [b]	dcm, tbah/Pt		0.65	101
$[Ru(tbcq)(CO)_2(PPh_3)_2]$ [b]	dcm, tbah/Pt		0.66	101
$[Ru(bpy)_2(dbcq)]$	dce, tbap/Pt	0.15	−0.75	104
$[Ru(bpy)_2(Hcq)]$	dce, tbap/Pt	0.31	−0.57	104
$[Ru(bpy)_2(tccq)]$	dce, tbap/Pt	0.64	−0.22	104
$[Ru(py)_4(dbcq)]$	dce, tbap/Pt	0.16	−0.84	104
$[Ru(py)_4(tccq)]$	dce, tbap/Pt	0.70	−0.33	104

[a] The **R** substituents (abbreviations given in parentheses) of structure **29** are **R** = 3,5-di-*t*-butyl (db), **R** = H (H), **R** = 3,4,5,6-tetrachloro (tc) and **R** = 3,4,5,6-tetrabromo (tb).

[b] A reversible one-electron transfer at ca. 1.7 V is observed but the origin has not been assigned.

oxidation state of the ligand in relation to that of the metal centre. In this regard, the case of 3*d* ions is well developed but much remains to be done for 4*d* and 5*d* ions [98–100].

The case of ruthenium is documented in a few publications [101–106]. The available information can be qualitatively unified on the basis of the following simple principles. In the presence of strongly π-accepting coligands (CO, PPh_3, bpy etc.) in sufficient numbers, the ruthenium(II) state is stabilized and can support the chelation of **29** in its various oxidation levels. Here redox processes, except possibly those occurring at very high and very low potentials, would primarily involve the quinonoid system. However, when π acceptance by coligands is limited, possible changes in the oxidation levels of the metal and/or ligand must be taken into account. Here it may be expected that **29** would bind to ruthenium(II) in the π-accepting Rq form and to higher oxidation states of the metal in the electron-rich reduced forms, Rsq and Rcq.

(c) When coligands are not strong π acceptors

We shall consider examples of the second situation first. Ammonia is not a π acceptor and it affords genuine (spectroscopic and magnetic data) Ru^{III}Rcq complexes of type **30a** which can be reversibly oxidized electrochemically or chemically [103]. The product of this one-electron oxidation was diagnosed as an Ru^{II}Rq complex (**30b**) primarily on the basis of carbonyl stretch data. If this is true, the oxidation **30a** → **30b** (E°_{298}, 0.1–0.4 V) is the net result of a two-electron oxidation of the ligand and a one-electron reduction of the metal.

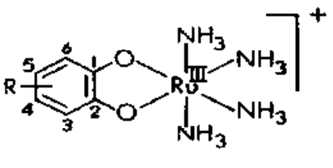

R = H, 4-CO_2H, 4-$CH_2CH_2CO_2H$,
4,5-benzo

30a

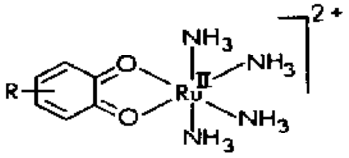

30b

The structure (**31**) of an $[RuL_2(O,O)_2]$ complex derived from 3,5-di-*t*-butylquinone is known (L = 4-*t*-butylpyridine) [105,106]. The C–O lengths in a coordinated quinonoid system are a good indication of the latter's oxidation state: Rq, 1.23 Å; Rsq, 1.29 Å; Rcq, 1.34 Å [98,106]. In **31** the C–O distance is 1.321(5) Å, a value intermediate between the lengths associated with Rsq and Rcq. The ruthenium oxidation state is a hybrid of +2 and +4.

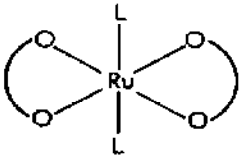

31

(d) When coligands are strongly π accepting

We can now summarize the cases where strong π-accepting coligands are abundantly present. At present this group consists of two varieties: carbonyl–phosphine mixed complexes and bpy complexes. Tetrachloro and tetrabromo quinones oxidatively add to $[Ru(CO)_3(PPh_3)_2]$ affording orange complexes of type **32a** [101]. These can be reversibly oxidized electrochemically (Table 7) and chemically, furnishing the semiquinone congener **32b**. EPR results reveal that in **32b** the unpaired electron is essentially Rsq in character, but it is subject to slight delocalization at least over the ruthenium and phosphorus atoms. As for free Rsq [94], the isotropic g values for **32b** in dichloromethane lie close to 2.00 but with a small ^{31}P coupling ($A \approx 25$ G). In frozen solution (77 K), only a very small g anisotropy is observed ($g_\perp = 2.02$, $g_\parallel = 2.00$, tetrabromo complex). In genuine ruthenium(III) complexes the anisotropy is much larger as in **30a** ($R = 4\text{-}CO_2H$; $g_\perp = 2.72$, $g_\parallel = 1.89$) [103]. The $Ru^{III}Rcq$ character of **32b** is significant but small.

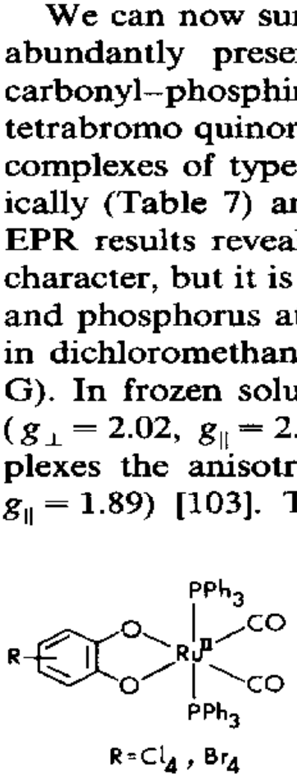

32a

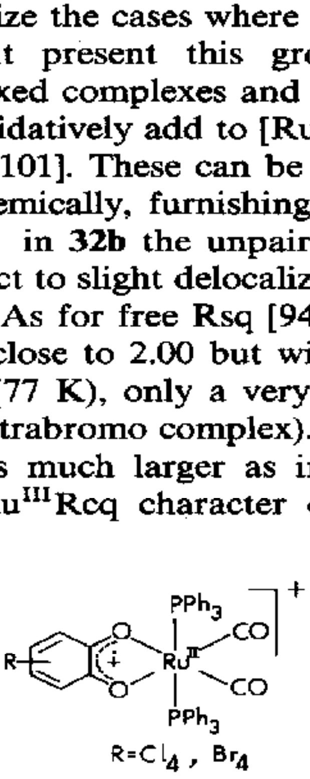

32b

Complexes closely related to **32** have also been described [102].

Complexes of type $[Ru(bpy)_2(Rcq)]$ (**33a**) and $[Ru(py)_4(Rcq)]$ have been isolated in the pure state [104]. These display two successive and reversible one-electron oxidations (Table 7) attributed to changes in the quinonoid fragment:

$$[Ru^{II}Rq] \underset{-e^-}{\overset{+e^-}{\rightleftharpoons}} [Ru^{II}Rsq] \underset{-e^-}{\overset{+e^-}{\rightleftharpoons}} [Ru^{II}Rcq] \tag{26}$$

where the $(bpy)_2$ or $(py)_4$ moieties are not shown. The Rsq complex **33b** has been isolated as salts via aerial oxidation of the **33a** congener. Other Rsq and Rq species can be generated in solution coulometrically. The status of

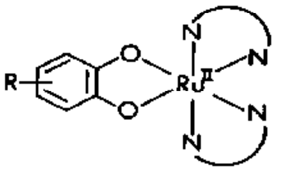

33a

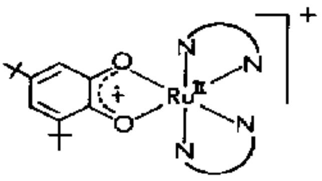

33b

the unpaired electron in **33b**, as revealed by EPR spectra, is similar to that in **32b**. The X-ray structure of the perchlorate salt of **32b** is known [106]. Here the two C–O distances are unfortunately unequal. One of these is 1.289(14) Å and is compatible with the Rsq formulation of **33b**. The other distance is longer, 1.327(15) Å, apparently due to certain intermolecular contacts. This complication makes a confident designation of the oxidation state difficult. In another member of this family, such a difficulty may not arise, and a structure solution of such a system would clarify matters. Ideally, structural information for all the three members in eqn. (26) would be desirable. More work on ruthenium–quinonoid systems is required. It is hoped that the principles enunciated earlier will provide a basis for further research.

(vii) Flavins

(a) Free ligands

Variable oxidation states of prosthetic groups provide the key to the functioning of redox enzymes. Such groups usually contain transition metal ions and/or certain unsaturated organic molecules such as flavins in flavoproteins [107,108]. Flavins, exemplified in **34**, are substituted isoalloxazines. The best known flavin is riboflavin (vitamin B_2), **34c**. The parent isoalloxazine (R, R′ and R″ in **34** replaced by H) tautomerizes immediately to alloxazine by a 10 → 1 prototropic shift. The 10-R substituent is crucial for stabilizing the isoalloxazine tautomer.

The isoalloxazine ring in **34** is in the most oxidized form, the quinonoid (fq) form. The semiquinone (fsq) and the hydroquinone (fhq) forms are

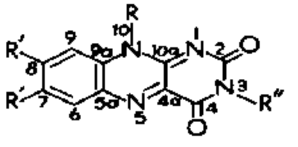

34

Ligand	R″	R′	R
34a	H	H	Me
34b	Me	H	Me
34c	H	Me	$CH_2(CHOH)_3CH_2OH$
34d	H	Me	Me

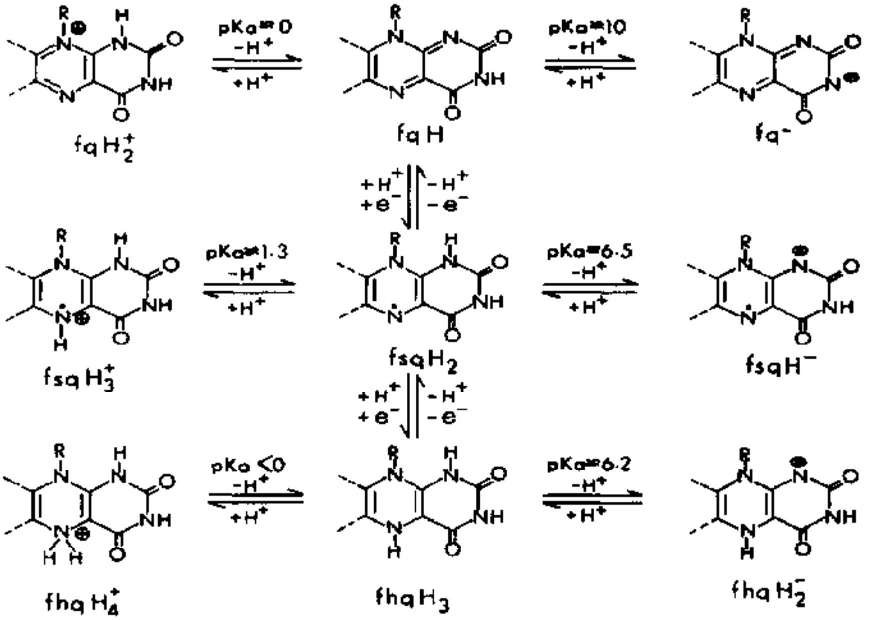

Fig. 8. The flavin redox system (only the pyrimidinoid part is shown) (adapted from Angew. Chem., Int. Ed. Engl., 4 (1965) 671).

derived from it by successive one-electron reductions. However, in protic media the electron transfer behaviour of flavins is complicated by simultaneous proton transfer involving the basic nitrogen centres. Each of the three oxidation states can be envisaged in cationic, neutral and anionic forms, depending on pH. In principle, this can afford an array of electroprotic equilibria [109] as depicted in Fig. 8. Structural studies [110–114] have revealed that the quinonoid ring system (Fig. 8) is nearly planar, the fully reduced $fhqH_3$ system is folded about the N(5)–N(10) axis and the semiquinone form $fsqH_2$ is probably also folded, though to a lesser extent. The fold is interrelated to the localization of the C(4a)–C(10a) double bond and tetrahedral hybridization of the N(5) and N(10) atoms. The EPR spectra of semiquinone species (generated by chemical reduction) correspond to localization of spin density, primarily at N(5) [115,116].

The variable-pH polarographic reduction of riboflavin at a dropping mercury electrode in aqueous solution was studied by Brdička and others many years ago and the results have been reviewed [117,118]. A two-electron wave, believed to be the result of two overlapping one-electron processes (quinone → semiquinone → hydroquinone), is observed throughout the pH range. The half-wave potential is pH dependent, owing to the involvement of protons in the redox equilibria (Fig. 8). Two changes in the slope of a linear $E_{1/2}$–pH plot occur at pH ca. 6 and ca. 10, corresponding to the acid dissociation constants of $fhqH_3$ and fqH respectively.

In aprotic non-aqueous media, the electrochemical behaviour is quite different, and the semiquinone form can be separately generated and directly observed. Riboflavin has been examined in dmso at both mercury [118,119] and platinum [120] electrodes. In neutral dmso solution, a quasi-reversible one-electron cyclic voltammetric couple (E_{pc}, −0.82 V; E_{pa}, −0.55 V) corresponding to the formation of the semiquinone radical anion (Fig. 8) is observed at a platinum electrode. The anion can be generated coulometrically (−0.9 V) and is stable for several hours in the absence of oxygen. A second reduction is observed at −1.3 V but its chemical nature is unclear [120].

(b) Complexes

Generally, flavoquinones (**34**) are poor coordinating agents for metal ions. The electron pair at N(5) is not sufficiently basic, and 3,4-prototropy which could convert **34** into an 8-hydroxyquinoline-like reagent is energetically unfavourable [121]. Ruthenium(II) is an exception, and dark blue stable complexes of type $[Ru^{II}(NH_3)_4(fq)]^{2+}$ can be readily obtained and have been described for the ligands **34a**–**34c** [113,122–124]. Structural work on the complex with fq = **34a** has revealed metal binding at N(5) and O at C(4) as in **35**. The special stabilizing factor for the structure appears to be strong ruthenium(II)–fq π-backbonding. Owing to this electron flow, bound fq develops an approximately 10° fold along the N(5)–N(10) axis. The free ligand is planar [110]. It appears as though the bound ligand exists in a partially reduced state. The cyclic voltammetry of **35** has been reported in both non-aqueous [121] and aqueous [113,122,123] media. A one-electron metal oxidation couple is seen at positive potentials. However, the most remarkable feature is the observation of two distinct one-electron responses on the negative side of the SCE assignable to the complexed quinone/semiquinone and semiquinone/hydroquinone couples in neutral dmf as well as in alkaline aqueous solution. Below we consider in some detail the results obtained in buffered aqueous solution.

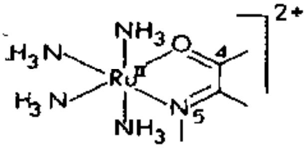

35

Owing to rapid proton-assisted dissociation of the hydroquinone com-

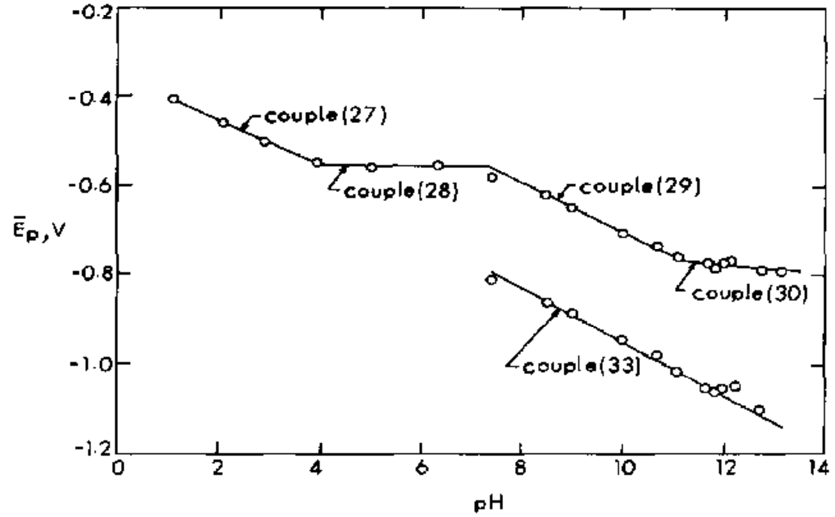

Fig. 9. $\overline{E}_p$–pH plots for the riboflavin complex of tetraammineruthenium(II) (adapted from ref. 123).

plexes below pH 7, the complexed semiquinone/hydroquinone couple is not observable at acidic pH. The semiquinone complexes are also unstable at low pH owing to competition for the N(5) site by protons. However, by increasing the scan rate, it is still possible to observe the complexed quinone/semiquinone couple under acidic conditions. The observed $\overline{E}_p$–pH plots for the riboflavin complex are displayed in Fig. 9.

The behaviour of the complexed quinone/semiquinone couple can be rationalized with the help of the following dissociation constants (pK): Ru(ribqH$_2^+$), 0.7 ± 0.1 (dissociation of proton at N(1)); Ru(ribqH), 7.4 ± 0.1 (N(3)); Ru(ribsqH$_2$), 3.98 ± 0.09 (N(1)) and Ru(ribsqH$^-$), 10.9 ± 0.2 (N(3)). Here ribqH$_2^+$ etc. has the same meaning as in Fig. 8 but with specific reference to riboflavin. For brevity, the coordinated NH$_3$ ligand and net charge on the complexes are not shown. The equilibria at the electrode in various pH ranges are as follows.

For 1 < pH < 4, H$^+$ transfer site N(1)

$$\mathrm{Ru(ribqH)} + \mathrm{H}^+ + \mathrm{e}^- \rightleftharpoons \mathrm{Ru(ribsqH_2)} \tag{27}$$

For 4 < pH < 7

$$\mathrm{Ru(ribqH)} + \mathrm{e}^- \rightleftharpoons \mathrm{Ru(ribsqH^-)} \tag{28}$$

For 7 < pH < 11, H$^+$ transfer site N(3)

$$\mathrm{Ru(ribq^-)} + \mathrm{H}^+ + \mathrm{e}^- \rightleftharpoons \mathrm{Ru(ribsqH^-)} \tag{29}$$

For 11 < pH < 13

$$\mathrm{Ru(ribq^-) + e^- \rightleftharpoons Ru(ribsq^{2-})} \quad (30)$$

The E°_{298} values of the electroprotic couples (27) and (29), calculated with the help of eqn. (31) [109]

$$E^\circ_{298} = \bar{E}_p + 0.059\mathrm{pH} \quad (31)$$

and the data in Fig. 9, are approximately −0.33 V and −0.12 V respectively. The pH-independent couples (28) and (30) have E°_{298} values of −0.56 and −0.79 V respectively. The E°_{298} values of couples (27) and (28), and of (29) and (30) are interconverted using eqn. (32) [109]:

$$(E^\circ_{298})_i = (E^\circ_{298})_j + 0.059\mathrm{p}K \quad (32)$$

Using the E°_{298} and pK values stated above ($i = 27$, $j = 28$, pK 3.98 and $i = 29$, $j = 30$, pK 11.9), it is seen that the above relation holds satisfactorily.

The observed pH-dependence (ca. 60 mV shift in $\bar{E}_p$ for unit change in pH) of the complexed semiquinone/hydroquinone couple above pH 7 corresponds to the transfer of one proton at the N(1) site (estimated pK 11.5) (couple (33)):

$$\mathrm{Ru(ribsqH^-) + H^+ + e^- \rightleftharpoons Ru(ribhqH_2^-)} \quad (33)$$

The E°_{298} of this couple is estimated (eqn. (31), Fig. 9) to be −0.36 V.

The electrochemistry of ruthenium-coordinated flavins in aqueous solution differs from that of free flavins in the same solvent in two significant ways. In the latter, a two-electron process is observed throughout the pH range. In the former the three oxidation states of the flavin moiety become directly observable. In free flavins, the response potentials are pH dependent over the entire range, but in the complexes, there are pH regions where proton transfer is absent. The blocking of the N(5) site by coordination and changes in the flavin pK values upon coordination make this possible. Owing to extensive backbonding, ruthenium-coordinated flavins are more difficult to reduce than free flavins. The opposite relationship usually applies to the other ligands considered in this article.

(viii) Porphyrins

(a) Free ligands

Porphyrins (**36**) are of great interest in biology, and their oxidation states in the free and complexed forms have been the subject of numerous studies [125]. Porphyrins will be generally abbreviated as H_2pp where H refers to dissociable NH hydrogen. Some specific abbreviations are also shown in **36**. Both the highest occupied and lowest unoccupied π-MOs of the highly

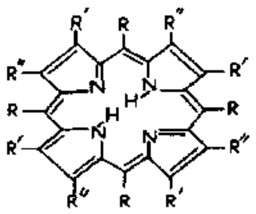

R	R′	R″	Abbreviation
H	C_2H_5	C_2H_5	H_2oep
H	C_2H_5	CH_3	H_2etp
C_6H_5	H	H	H_2tpp
p-XC_6H_4	H	H	H_2Xtpp

36

conjugated ligand frame are electrochemically accessible in non-aqueous media, affording five oxidation levels in all (eqns. (34)–(37)):

$$[H_2pp]^{2+} + e^- \rightleftharpoons [H_2pp]^+ \tag{34}$$

$$[H_2pp]^+ + e^- \rightleftharpoons [H_2pp] \tag{35}$$

$$[H_2pp] + e^- \rightleftharpoons [H_2pp]^- \tag{36}$$

$$[H_2pp]^- + e^- \rightleftharpoons [H_2pp]^{2-} \tag{37}$$

where $[H_2pp]^+$ is a π-cation radical, $[H_2pp]^{2+}$ a π dication, $[H_2pp]^-$ a π-anion radical and $[H_2pp]^{2-}$ a π dianion [126–132]. In favourable cases, all the four couples corresponding to eqns. (34)–(37) are experimentally observable. Representative formal potential data are shown in Table 8. Certain regularities in the relative values of formal potentials among porphyrins and their metal complexes are evident [131,133]:

$$E^\circ(34) - E^\circ(35) = 0.3 \pm 0.1 \text{ V}$$

$$E^\circ(35) - E^\circ(36) = 2.25 \pm 0.15 \text{ V}$$

$$E^\circ(36) - E^\circ(37) = 0.4 \pm 0.1 \text{ V}$$

The difference $E^\circ(35) - E^\circ(36)$ is an approximate measure of the first π–π^* transition energy. The dependence of the formal potentials of eqns. (34)–(37) on substituents and solvents has been investigated [132].

(b) Role of axial ligands in complexes

Transition metal ions are usually bound by porphyrins in the deprotonated form (pp^{2-}) with the help of the planar N_4 matrix. The two *trans* axial sites can be utilized for ligand binding. Depending on the *trans*-labilizing powers of the ligands and on other factors, one or both *trans* positions may be occupied, leading to grossly square-pyramidal (**37**) or octahedral (**38**)

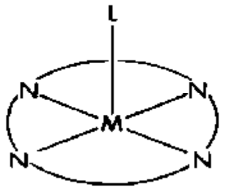

37

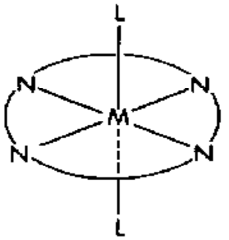

38

geometries. In the absence of ligation, the axial sites can promote metal–metal binding particularly in the case of heavy metals [134]. Such axial phenomena can profoundly influence the electronic properties of the coordinated macrocycle, including the accessibility of porphyrin oxidation states in relation to those of the metal. Ruthenium porphyrins provide model examples.

Ruthenium is generally inserted into porphyrins as the carbonyl fragment Ru(II)CO [135–137]. Some reactions affording [138–144] different types of ruthenium porphyrins are stated in eqns. (38)–(42):

$$[\mathrm{Ru^{II}(pp)(CO)}] \xrightarrow{\mathrm{L}} [\mathrm{Ru^{II}(pp)(CO)L}] \tag{38}$$

$$[\mathrm{Ru^{II}(pp)(CO)py}] \xrightarrow{\mathrm{py},\, h\nu} [\mathrm{Ru^{II}(pp)(py)_2}] \tag{39}$$

$$[\mathrm{Ru^{II}(pp)(CO)(EtOH)}] \xrightarrow{\mathrm{PR_3}} [\mathrm{Ru^{II}(pp)(PR_3)_2}] \tag{40}$$

$$[\mathrm{Ru^{II}(pp)(CO)}] \xrightarrow{t\text{-BuOOH}} [\mathrm{Ru^{IV}(pp)(OH)_2}]_2\mathrm{O} \tag{41}$$

$$[\mathrm{Ru^{II}(pp)(py)_2}] \xrightarrow{\text{vacuum}} [\mathrm{Ru_2^{II}(pp)_2}] \tag{42}$$

In eqn. (38), L can be chosen from a wide variety of donors such as EtOH, tetrahydrofuran, dmso, py, MeCN etc. The complex [Ru(pp)(CO)] belongs to the structural type **37** while [Ru(pp)(CO)L], [Ru(pp)(py)$_2$] and [Ru(pp)(PR$_3$)$_2$] belong to type **38**. The structures of [Ru(tpp)(CO)L], L = py and EtOH, are known [145,146]. The species of type [Ru(pp)(OH)]$_2$O has a linear Ru^{IV}–O–Ru^{IV} bridge (**39**) and the porphyrin rings are staggered with respect to each other [142,144]. The dimer [Ru$_2$(pp)$_2$] (**40**) also has staggered

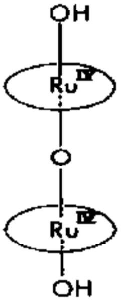

39

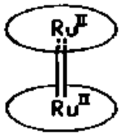

40

TABLE 8

Porphyrins

Species [a]	Conditions	E°_{298} (V)			Ref.
		Ligand		Metal	
		Reduction	Oxidation	Oxidation	
H_2oep	dcm, tbah/Pt		0.83, 1.39		149
	dmso, teap/Pt	−1.86, −1.46			131
H_2etp	dcm, tbah/Pt		0.78, 1.34		149
H_2tpp	dcm, tbah/Pt		0.95, 1.28		149
	dcm, tbap/Pt	−1.55, −1.20	1.02, (1.24) [b]		132
[Ru(oep)(CO)]	dcm, tbah/Pt		0.64	1.21	149
[Ru(etp)(CO)]	dcm, tbah/Pt		0.61	1.11	149
[Ru(tpp)(CO)py]	dcm, tbah/Pt		0.81	1.36	149
	py, tbap/Pt	−1.39	1.02		153
[Ru(tpp)(CO)(dmso)]	dmso, tbap/Pt	−1.81, −1.35	0.99		153
[Ru(*p*-MeOtpp)(CO)]	dcm, tbah/Pt		0.74	1.18	151
	dmso, tbah/Pt	−1.35			151
[Ru(*p*-Metpp)(CO)]	dcm, tbah/Pt		0.75	1.20	151
	dmso, tbah/Pt	−1.35			151
[Ru(tpp)(CO)]	dcm, tbah/Pt		0.79	1.20	151
	dmso, tbah/Pt	−1.32			151

[Ru(*p*-Ftpp)(CO)]	dcm, tbah/Pt		0.85	1.25	151
	dmso, tbah/Pt	−1.28			151
[Ru(*p*-Cltpp)(CO)]	dcm, tbah/Pt		0.86	1.27	151
	dmso, tbah/Pt	−1.24			151
[Ru(*p*-Brtpp)(CO)]	dcm, tbah/Pt		0.86	1.25	151
	dmso, tbah/Pt	−1.24			151
[Ru(*p*-Et_2Ntpp)(CO)(4-*t*-Bupy)]	dcm, tbap/Pt	−1.62	0.50, 0.73	1.06	155
[Ru(*p*-MeOtpp)(CO)(4-*t*-Bupy)]	dcm, tbap/Pt	−1.56	0.78	1.28	155
[Ru(*p*-Metpp)(CO)(4-*t*-Bupy)]	dcm, tbap/Pt	−1.54	0.81	1.32	155
[Ru(*p*-Prtpp)(CO)(4-*t*-Bupy)]	dcm, tbap/Pt	−1.54	0.85	1.33	155
[Ru(*p*-Cltpp)(CO)(4-*t*-Bupy)]	dcm, tbap/Pt	−1.46	0.95	1.43	155
[Ru(*p*-CF_3tpp)(CO)(4-*t*-Bupy)]	dcm, tbap/Pt	−1.39	1.04	1.47	155
[Ru(tpp)$(py)_2$]	dcm, tbah/Pt		1.26	0.21	149
[Ru(oep)$(PBu_3)_2$]	dcm, tbah/Pt		1.16	−0.01	140
[Ru(oep)(py)(MeCN)]	dcm, tbah/Pt		1.05	0.08	149

[a] 4-*t*-Bupy = 4-tert-butylpyridine.

[b] Estimated from Fig. 1 of ref. 132.

porphyrin rings [147]. The metal–metal double bond holds two unpaired electrons ($\sigma^2\pi^4n^4\pi^{*2}$) [148].

The first report on the electrochemistry of ruthenium porphyrins appeared in 1973 [149]. This work was concerned with cyclic voltammetric and coulometric oxidations of species of types [Ru(pp)(CO)], [Ru(pp)(CO)py], [Ru(pp)(py)$_2$] etc. and laid the foundation of subsequent activities [140,150–155].

In carbonyl complexes of types **37** and **38**, there is strong axial π-backbonding involving metal d_{xz}, d_{yz} and π^*(CO). This is reflected in low ν_{CO} values, 1920–1930 cm^{-1} [149,150]. A secondary effect of this binding is *trans* labilization. Thus [Ru(pp)(CO)] exists as such in non-coordinating solvents, while in coordinating solvents or in the presence of donor ligands, the *trans* position becomes occupied (see eqn. (38)) but relatively weakly [145,146,156]. Extended Hückel calculations on [Ru(oep)(CO)py] have revealed that owing to axial backbonding the filled metal π orbitals are significantly stabilized to make a porphyrin orbital of $a_{2u}(\pi)$ symmetry, the highest occupied molecular orbital (HOMO). The LUMO is also a porphyrin orbital, $e_g(\pi^*)$ [139]. Thus one-electron oxidation and one-electron reduction of the carbonyl complexes should both involve the porphyrin ligand rather than the metal centre. This is in accord with experimental results.

In non-carbonyl species, axial backbonding is relatively weak or absent. A metal orbital now becomes the HOMO lying above $a_{2u}(\pi)$. The LUMO remains $e_g(\pi^*)$ as before. Here the first oxidation is expected to occur at the metal, as found in practice.

(c) Carbonyl complexes

In general, cyclic voltammetry of such complexes reveals two successive one-electron oxidative responses in dcm solution (Fig. 10); for [Ru(Xtpp)(CO)L] a one-electron reduction is also observable [140,149,151, 153,155]. All the responses are more or less reversible on the cyclic voltammetric time scale. Selected formal potential data are listed in Table 8.

The monocations [Ru(pp)(CO)L$_n$]$^+$ ($n = 0, 1$) produced by the first oxidation are chemically quite stable and can be prepared in solution by electro-oxidation. However, the dicationic product of the second oxidation is stable only on the cyclic voltammetric time scale. Attempts to generate solutions of the dication have not been successful, and the same is true for the monoanion [Ru(Xtpp)(CO)L]$^-$ formed by one-electron reduction.

The EPR spectra of the monocation [Ru(pp)(CO)L$_n$]$^+$ ($n = 0, 1$) taken in frozen solution (77 K) consist of an isotropic signal at $g = 2.00$. The ν_{CO} band of the oxidized complex is shifted by 15–30 cm^{-1} from that of the parent complex. This shift is much smaller than that expected ($\geqslant 100$ cm^{-1}) for metal oxidation. Thus the redox orbital involved in the first oxidation is

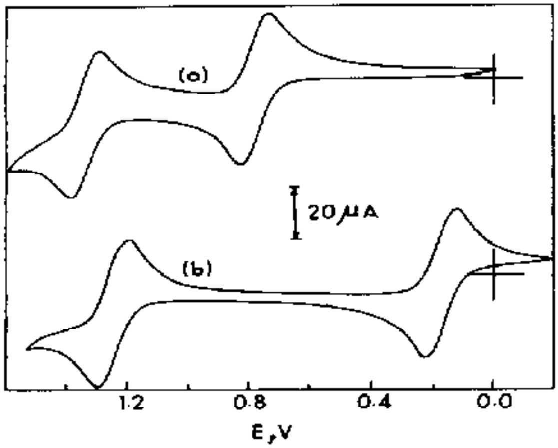

Fig. 10. Cyclic voltammograms (dcm, tbah/Pt) of (a) [Ru(tpp)(CO)py] and [Ru(tpp)(py)$_2$] at 298 K (adapted from ref. 149).

porphyrin based. The visible spectrum of the monocation also supports this conclusion [149,155]. The redox couple corresponding to the first oxidation is thus given by eqn. (43):

$$[\mathrm{Ru^{II}(pp^{+\bullet})(CO)L}_n]^+ + \mathrm{e}^- \rightleftharpoons [\mathrm{Ru^{II}(pp)(CO)L}_n] \qquad (43)$$

The reduction potentials for the first oxidation (in dcm containing one molar L) in a series of complexes of type [Ru(tpp)(CO)L], where L is py or substituted derivatives thereof, have been reported [154]. The pK_a of the conjugate acid of L (in aqueous solution) was varied over a wide range (0.67–6.46) and the E° values decreased from 0.95 to 0.86 V. The potentials correlate linearly with pK_a. The equilibrium constants for the reactions (eqns. (44) and (45))

$$[\mathrm{Ru(tpp)(CO)}] + \mathrm{L} \rightleftharpoons [\mathrm{Ru(tpp)(CO)L}] \qquad (44)$$

$$[\mathrm{Ru(tpp)(CO)}]^+ + \mathrm{L} \rightleftharpoons [\mathrm{Ru(tpp)(CO)L}]^+ \qquad (45)$$

have also been determined in dcm solution containing a suitable concentration of L. The stability constants of the two equilibria have very similar values. That is why the shift in potential on going from [Ru(tpp)(CO)] to the pyridine adducts [Ru(tpp)(CO)L] is small (100 mV or less). A similar study has been conducted for the reaction of [Ru(tpp)(CO)] with a series of donor solvents (S) utilized as ligands in dcm. The reduction potentials of both the first oxidation [Ru(tpp)(CO)(S)]$^+$/[Ru(tpp)(CO)(S)] and the reduction [Ru(tpp)(CO)(S)]/[Ru(tpp)(CO)(S)]$^-$ could be correlated to solvent parameters [153].

The assignment of the redox orbital in the case of the second oxidation is less certain, but the balance of evidence [151,155] suggests that it is metal centred as shown in eqn. (46):

$$[\mathrm{Ru^{III}(pp^{+\cdot})(CO)L}_n]^{2+} + e^- \rightleftharpoons [\mathrm{Ru^{II}(pp^{+\cdot})(CO)L}_n]^{+} \qquad (46)$$

One of the arguments in favour is that the difference in potentials between the first and the second oxidation steps (Table 8) is substantially larger than 0.3 V found [131] in porphyrins and metalloporphyrins where both oxidations are genuinely porphyrin based. A second line of evidence is based on substituent effects (see below). On a similar basis, the redox orbital in the one-electron reduction is believed to be porphyrin based [151,155]. This is shown in eqn. (47):

$$[\mathrm{Ru^{II}(Xtpp)(CO)}] + e^- \rightleftharpoons [\mathrm{Ru^{II}(Xtpp^{-\cdot})(CO)}]^{-} \qquad (47)$$

The effect of substituent X (MeO, Me, H, F, Cl, Br) on the reduction potentials of [Ru(Xtpp)(CO)] has been assessed [151]. Oxidations were studied in dcm and reductions in dmso; the species undergoing reduction is thus [Ru(Xtpp)(CO)(dmso)]. Data are collected in Table 8. The reduction potentials of all three couples (eqns. (43), (46) and (47)) correlate linearly with $4\sigma_X$ where σ_X is the Hammett constant of substituent X and the factor 4 appears owing to the presence of the four X substituents. The relationship

$$\Delta E_T^\circ = 4\sigma_X\rho \qquad (48)$$

holds. Here ρ is the reaction constant measuring the susceptibility of the electron-transfer process to polar effects and ΔE_T° is the shift of E_T° from the X = H case. The values of ρ, obtained as the slope of the plot of E_T° vs. $4\sigma_X$, are as follows: first oxidation (eqn. (43)), 0.066 V; second oxidation (eqn. (46)), 0.041 V; first reduction (eqn. (47)), 0.064 V. The ρ value for the second oxidation is significantly lower than that for the first oxidation whose ρ value is close to that for the first reduction. In a general way, the more remote the redox orbital is from X, the less ρ should be. On this basis, the assignments of redox orbitals as made in eqns. (43), (46) and (47) are consistent with the ρ values. More complex substituent effects are reported for [Ru(Xtpp)(CO)(*t*-Bupy)] (X = Et_2N, MeO, Me, *n*-Pr, Cl, CF_3) studied in dcm [155]. A notable result is that the complex with X = Et_2N displays three reversible oxidations (E_{298}°, 0.50, 0.73 and 1.06 V) instead of the usual two; however, only one reduction (E_{298}°, −1.62 V) is observed as in the other cases. The first two of the three successive oxidations for the X = Et_2N case are attributed to porphyrin oxidations and the third to metal oxidation.

(d) Non-carbonyl complexes

Selected examples together with formal potential data are given in Table 8. Like the carbonyl complexes, these also display two reversible to quasi-reversible one-electron oxidations in dcm solutions (Fig. 10). However, the separation between the two responses is substantially larger in the non-carbonyl species primarily because the first oxidation occurs at much lower potential. Thus the difference in the E°_{298} values of the first oxidations of [Ru(tpp)(CO)py] and $[\mathrm{Ru(tpp)(py)_2}]$ is 0.6 V. The monocation produced coulometrically is quite stable in solution and its electronic spectrum is closely similar to that of iron(III) porphinate. Indications are strong that it is a ruthenium(III) complex. Unfortunately, it is EPR silent even in frozen solution (77 K) but this can be due to rapid relaxation of the low spin d^5 ion. It is generally agreed that the two oxidations correspond to the processes of eqns. (49) and (50):

$$[\mathrm{Ru^{III}(tpp)(py)_2}]^{+} + e^{-} \rightleftharpoons [\mathrm{Ru^{II}(tpp)(py)_2}] \tag{49}$$

$$[\mathrm{Ru^{III}(tpp^{+\cdot})(py)_2}]^{2+} + e^{-} \rightleftharpoons [\mathrm{Ru^{III}(tpp)(py)_2}]^{+} \tag{50}$$

in which the metal and the ligand are oxidized in that sequence [149].

The electrochemical behaviour of complexes with axial tertiary phosphines [140,152] has been studied. Complex $[\mathrm{Ru(oep)(PBu_3)_2}]$ follows the pattern of eqns. (49) and (50). In this case the $[\mathrm{Ru^{III}(oep)(PBu_3)_2}]^+$ cation can be isolated as the bromide salt via dibromine oxidation of the parent complex. Further, the product of the second oxidation, namely $[\mathrm{Ru^{III}(oep^{+\cdot})(PBu_3)_2}]^{2+}$, is EPR active in frozen solution (77 K). Two signals of nearly equal intensity are observed at $g = 2.35$ (broad) and $g = 2.008$ (sharp). These have been assigned respectively to the ruthenium(III) and porphyrin radical. The assumption is that there is no serious coupling between the two paramagnetic centres of the dication. Further EPR work on the ruthenium(III) species considered in this section is required.

An interesting reaction occurs upon adding $\mathrm{PBu_3}$ or $\mathrm{PPh_3}$ to the $[\mathrm{Ru^{II}(oep^{+\cdot})(CO)(py)}]^+$ cation in solution:

$$[\mathrm{Ru^{II}(oep^{+\cdot})(CO)(py)}]^{+} + 2\mathrm{PPh_3} \longrightarrow [\mathrm{Ru^{III}(oep)(PPh_3)_2}]^{+} + \mathrm{CO} + \mathrm{py} \tag{51}$$

Apparently an internal electron transfer from ruthenium(II) to the bound porphyrin radical occurs following loss of the CO ligand. The reaction in eqn. (51) succinctly embodies the basic difference between the redox orbitals of the carbonyl and non-carbonyl monocations.

(e) Dimeric complexes

We first consider the oxo-bridged dimer **39**. The cyclic voltammetry of $[\mathrm{Ru^{IV}(oep)X]_2O}$ has been examined in dcm [143]. Three quasi-reversible couples are observed, each corresponding to the transfer of two electrons. It has been suggested (but not proved) that the couples (the case of X = OH is chosen) are those shown in eqn. (52):

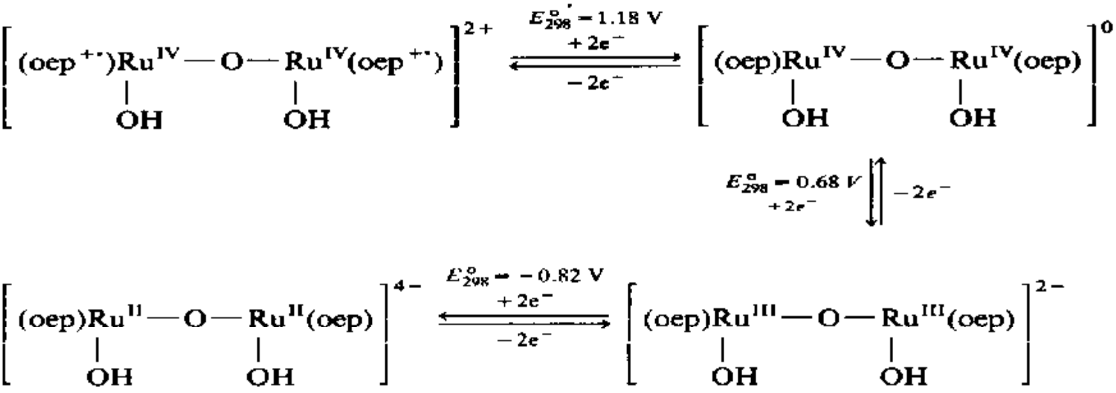

$$\begin{tikzcd}[column sep=huge] \left[(\mathrm{oep}^{+\cdot})\mathrm{Ru^{IV}}(\mathrm{OH})\text{—O—}\mathrm{Ru^{IV}}(\mathrm{OH})(\mathrm{oep}^{+\cdot})\right]^{2+} \arrow[r, shift left, "{E^{\circ\prime}_{298} = 1.18\ \mathrm{V}} \atop {+2e^-}"] & \left[(\mathrm{oep})\mathrm{Ru^{IV}}(\mathrm{OH})\text{—O—}\mathrm{Ru^{IV}}(\mathrm{OH})(\mathrm{oep})\right]^{0} \arrow[l, shift left, "-2e^-"] \arrow[d, shift right, "{E^{\circ}_{298} = 0.68\ V} \atop {+2e^-}"'] \\ \left[(\mathrm{oep})\mathrm{Ru^{II}}(\mathrm{OH})\text{—O—}\mathrm{Ru^{II}}(\mathrm{OH})(\mathrm{oep})\right]^{4-} \arrow[r, shift right, "-2e^-"'] & \left[(\mathrm{oep})\mathrm{Ru^{III}}(\mathrm{OH})\text{—O—}\mathrm{Ru^{III}}(\mathrm{OH})(\mathrm{oep})\right]^{2-} \arrow[l, shift right, "{E^{\circ}_{298} = -0.82\ \mathrm{V}} \atop {+2e^-}"'] \arrow[u, shift right, "-2e^-"'] \end{tikzcd} \qquad (52)$$

Two of these couples involve metal orbitals and one involves ligand orbitals. Here the ruthenium(IV)/ruthenium(III) couple lies at a lower potential than the porphyrin redox couple. The ruthenium(IV) oxidation state is particularly stabilized in the linear Ru–O–Ru configuration. It is, however, surprising that in a strongly coupled situation such as this, the two parts are systematically oxidized or reduced at the same potential.

An even more dramatic example of the stabilization of higher oxidation states of ruthenium in relation to that of porphyrin exists [157]. The oxo-bridged dimers, **39**, are formed by the reaction in eqn. (41). Application of this reaction (replacing *t*-BuOOH with *m*-chloroperbenzoic acid) to the α,β,ν,δ-tetramesityl porphyrin complex, [Ru(tmp)(CO)], however, affords the *trans* dioxo complex $[\mathrm{Ru^{VI}(O)_2(tmp)}]$. Here dimerization is precluded by the steric bulk of the mesityl functions. The +6 state of the metal is so stabilized by the two oxo groups that it is unable to oxidize tmp. In dcm, this complex displays a single reversible oxidation wave at 1.12 V, corresponding to the formation of the porphyrin cation radical:

$$[\mathrm{Ru^{VI}(O)_2(tmp^{+\cdot})}]^+ + e^- \rightleftharpoons [\mathrm{Ru^{VI}(O)_2(tmp)}] \qquad (53)$$

We now turn to the metal–metal-bonded dimer **40**. In dimethoxyethane, $[\mathrm{Ru_2^{II}(oep)_2}]$ has been examined by cyclic and rotating disk voltammetry. A redox series consisting of six reversible couples is observed. These correspond to two successive reductions of the porphyrin, two successive oxidations of the metal and finally two successive oxidations of the porphyrin as stated in eqn. (54):

$$\begin{aligned}
&[(\mathrm{oep}^{+\cdot})\mathrm{Ru}^{\mathrm{III}}\equiv\mathrm{Ru}^{\mathrm{III}}(\mathrm{oep}^{+\cdot})]^{4+} \overset{E^{\circ}_{298}=1.25\ \mathrm{V}}{\xrightleftharpoons[-e]{+e}} \\
&[(\mathrm{oep}^{+\cdot})\mathrm{Ru}^{\mathrm{III}}\equiv\mathrm{Ru}^{\mathrm{III}}(\mathrm{oep})]^{3+} \overset{E^{\circ}_{298}=1.10\ \mathrm{V}}{\xrightleftharpoons[-e^-]{+e^-}} \\
&[(\mathrm{oep})\mathrm{Ru}^{\mathrm{III}}\equiv\mathrm{Ru}^{\mathrm{III}}(\mathrm{oep})]^{2+} \overset{E^{\circ}_{298}=0.57\ \mathrm{V}}{\xrightleftharpoons[-e^-]{+e^-}} \\
&[(\mathrm{oep})\mathrm{Ru}^{\mathrm{III}}\dot{=}\mathrm{Ru}^{\mathrm{II}}(\mathrm{oep})]^{+} \overset{E^{\circ}_{298}=-0.06\ \mathrm{V}}{\xrightleftharpoons[-e^-]{+e^-}} \\
&[(\mathrm{oep})\mathrm{Ru}^{\mathrm{II}}=\mathrm{Ru}^{\mathrm{II}}(\mathrm{oep})] \overset{E^{\circ}_{298}=-0.97\ \mathrm{V}}{\xrightleftharpoons[-e^-]{+e^-}} \\
&[(\mathrm{oep}^{-\cdot})\mathrm{Ru}^{\mathrm{II}}=\mathrm{Ru}^{\mathrm{II}}(\mathrm{oep})]^{-} \overset{E^{\circ}_{298}=-1.46\ \mathrm{V}}{\xrightleftharpoons[-e^-]{+e^-}} [(\mathrm{oep}^{-\cdot})\mathrm{Ru}^{\mathrm{II}}=\mathrm{Ru}^{\mathrm{II}}(\mathrm{oep}^{-\cdot})]^{2-}
\end{aligned} \tag{54}$$

The assignments are based on a critical comparison with the known electrochemical behaviour of free porphyrins and mononuclear complexes [158]. In the oxidized species the metal–metal bond orders are 2.5 and 3 compared with 2 in **40** [148].

Finally, we consider the case of cofacial porphyrin dimers such as H_4dpa (**41**). The ruthenium complex $[Ru_2(dpa)(PPh_3)_2]$ (**42**) shows two two-electron ligand oxidations (0.61 and 0.78 V) and one two-electron metal oxidation (−0.17 V). However, $[Ru_2(dpa)(py)_4]$ (**43**) displays two successive one-electron ligand oxidations (0.96 and 1.01 V) and two successive metal oxidations (−0.22 and −0.11 V). Other related species have also been investigated [159].

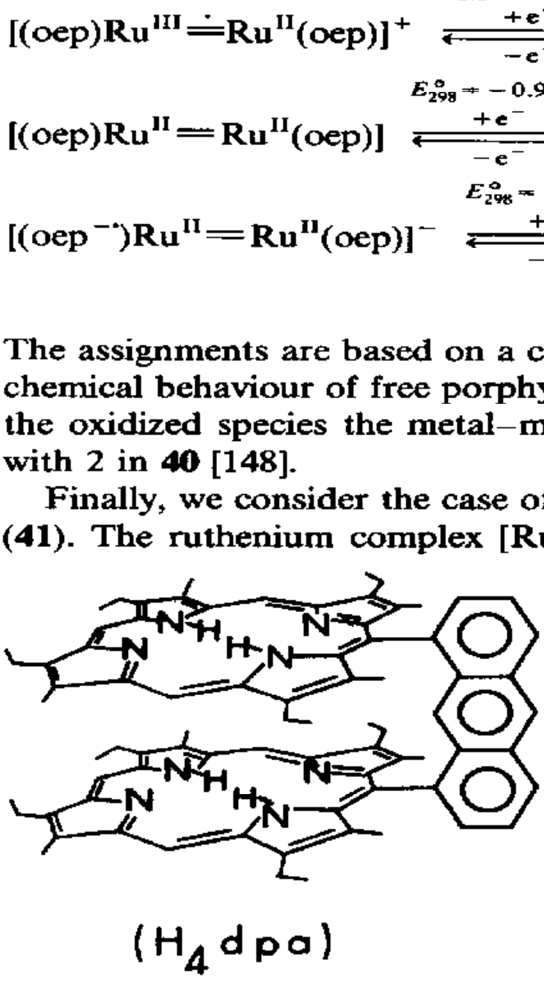

41

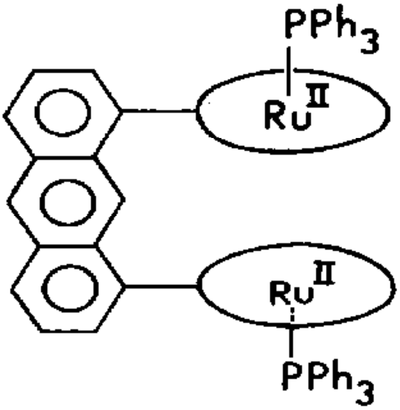

42

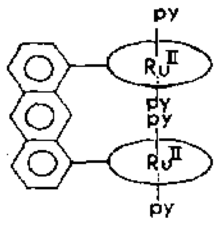

43

(ix) Phthalocyanines

(a) Free ligands

Phthalocyanine, H_2pc (**44**) is a tetrazaporphyrin: the methine and pyrrole functions of the porphyrin skeleton are replaced by nitrogen and benzpyrrole functions respectively. Like porphyrin, H_2pc acts as a planar N_4 macrocyclic ligand but with a smaller hole size [160–162]. Mild bases deprotonate phthalocyanine but not porphyrin, implying that the former is a weaker σ donor than the latter. However, phthalocyanine excels porphyrin as a π acceptor [163,164]. Both macrocycles have LUMOs of $e_g(\pi^*)$ symmetry. Stronger π acceptance by phthalocyanine is dependent on the greater stability of its LUMO and is reflected in (1) the higher reduction potentials of H_2pc and (2) superior π backbonding in Mpc compared with Mpp.

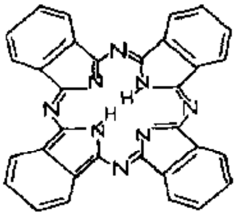

(H_2pc)

44

The insolubility of H_2pc has been a problem in electrochemical studies. However, by constant potential electrolysis in dmf, it can be solubilized, affording the radical anion $[H_2pc]^-$. Polarography of such solutions reveals four successive one-electron reductions:

$$[H_2pc] + e^- \rightleftharpoons [H_2pc]^- \tag{55}$$

$$[H_2pc]^- + e^- \rightleftharpoons [H_2pc]^{2-} \tag{56}$$

$$[H_2pc]^{2-} + e^- \rightleftharpoons [H_2pc]^{3-} \tag{57}$$

TABLE 9

Phthalocyanines

Species	Conditions	E°_{298} (V)		Ref.
		Ligand reduction	Ligand oxidation	
$[H_2pc]$	dmf, tpap/Hg	−0.66, −1.06, −1.93, −2.23		165
$Na_4[H_2pcts]$	dmso, teap/Hg	−0.52, −0.97, −1.81		166
$[Ru(pc)(py)_2]$	dcm, tbah/Pt		0.77, 1.40	175
$[Ru(pc)(4\text{-}Mepy)_2]$	dcm, tbah/Pt		0.74, 1.40	175
$[Ru(pc)(MeCN)_2]$	dcm, tbah/Pt		0.72	175
$[Ru(pc)(dmf)_2]$	dcm, tbah/Pt		0.80	175
$[Ru(pc)(dmso)_2]$	dcm, tbah/Pt		0.89	175
[Ru(pc)(CO)py]	dcm, tbah/Pt		0.91	175
[Ru(pc)(CO)(4-Mepy)]	dcm, tbah/Pt		0.88	175
[Ru(pc)(CO)(dmf)]	dcm, tbah/Pt		0.90	175

$$[H_2pc]^{3-} + e^- \rightleftharpoons [H_2pc]^{4-} \tag{58}$$

Formal potential data are given in Table 9. Complexes of type Mpc afforded by a bivalent metal behave similarly [161,165]. The polarography of the sodium salt of the tetrasulphonated derivative $Na_4[H_2pcts]$ has been reported in dmso at a rotating platinum electrode and a dropping mercury electrode. The reduction potentials are about 0.1 V higher than those of H_2pc. Three successive reductions are observable; the fourth is obscured by the onset of Na^+ reduction. Electrolysis of $Na_4[H_2pcts]$ at the potential of the first reduction plateau affords the radical anion $[H_2pcts]^{5-}$ having a strong EPR signal at $g = 2.00$ [166]. The observation of three to four successive reductions within the electrochemically accessible voltage domain reflects the relatively low energy of the LUMO in phthalocyanines. In the case of porphyrins, the LUMO energy is higher, and only the first two reductions are experimentally identifiable (compare Tables 8 and 9).

(b) Complexes

Blue phthalocyanine complexes of ruthenium(II) have been known for many years, but owing to synthetic difficulties, progress has been relatively slow [167–174]. The electrochemical oxidation of species of types [Ru(pc)(CO)L] and $[Ru(pc)(L)_2]$ has been studied in dcm [175,176]. These complexes are structural analogues of the corresponding porphyrin species (**38**) with the ligand pair CO,L or L,L axially coordinated to the Rupc plane.

The bis(pyridine) complexes show two reversible one-electron cyclic voltammetric oxidations; in the other complexes, only the first oxidation is observable (Table 9). The red-purple one-electron oxidized complexes can be produced in solution for all complexes by exhaustive electrolysis at the potential of the first oxidation. In frozen solution (77 K) an isotropic EPR signal near $g = 2$ is systematically observed for every complex. From this observation as well as from optical spectral data, it has been concluded [175] that both carbonyl and non-carbonyl species afford a coordinated phthalocyanine cation radical upon one-electron oxidation:

$$[Ru^{II}(pc^{+\cdot})(CO)L]^+ + e^- \rightleftharpoons [Ru^{II}(pc)(CO)L] \tag{59}$$

$$[Ru^{II}(pc^{+\cdot})(L)_2]^+ + e^- \rightleftharpoons [Ru^{II}(pc)(L)_2] \tag{60}$$

The site of the second oxidation in the bis(pyridine) complexes is, however, unknown; the dication is too unstable for generation by electrolysis. Cathodic reduction of the various complexes was also attempted, but no meaningful results could be obtained [175]. This is unfortunate since H_2pc itself displays a rich reduction series.

The porphyrin and phthalocyanine complexes are strikingly different with respect to the first oxidation. To highlight this, the behaviour of four specific

TABLE 10

Summary of oxidation behaviour of four porphyrin and phthalocyanine complexes

Complex	E°_{298} (V)	Oxidation site
[Ru(pc)(py)$_2$]	0.77	Ligand
[Ru(pc)(CO)py]	0.91	Ligand
[Ru(pp)(py)$_2$]	0.21	Metal
[Ru(pp)(CO)py]	0.81	Ligand

complexes is restated in Table 10. There is no qualitative difference between the oxidation sites of the non-carbonyl and carbonyl phthalocyanine species; only oxidation becomes a little more difficult (by 0.1 V) in the latter. Here the strong π-acceptor character of the macrocyclic ligand provides so much stability to the filled metal $d\pi$ orbital that the HOMO remains a phthalocyanine orbital irrespective of the nature of the axial ligands. In the case of porphyrins, the HOMO is a ligand orbital only when axial carbon monoxide is present for backbonding; otherwise it is a metal orbital. Hence there is the qualitative difference between the oxidation of [Ru(pp)(py)$_2$] and [Ru(pc)(py)$_2$].

The E°_{298} values of [Ru(pc)(CO)py] and [Ru(pp)(CO)py] suggest that the macrocyclic HOMO energies are not very different for the two ligands. The major difference between them lies in the π-backbonding interaction involving macrocycle LUMO and metal $d\pi$ orbitals, and in this property, phthalocyanine far excels porphyrin.

E. CONCLUDING REMARKS

In this article we have reviewed primarily the pattern and systematics of ligand redox in ruthenium complexes. The synergistic combination of electrochemical and spectroscopic methods has vastly increased our understanding of ligand redox phenomena during the last 15 years or so. This in turn has led to better understanding and new developments in other fields. Photophysics and photochemistry could be cited as examples [41]. We wish to mention specifically the area of catalysis and chemical reactivity. The reduced/oxidized ligands can act as reservoirs of electrons/holes and hence as centres which can support redox transformation of other chemical entities. We hope to cover this topic as a part of the next review.

ACKNOWLEDGEMENT

Financial support received from the Department of Science and Technology, the Council of Scientific and Industrial Research and the University Grants Commission, New Delhi, India, is gratefully acknowledged.

REFERENCES

1 J. Heyrovský and J. Kuta, Principles of Polarography, Academic Press, New York, 1966.
2 G. Charlot, J. Badoz-Lambling and B. Tremillon, Electrochemical Reactions, Elsevier, New York, 1962.
3 R.N. Adams, Electrochemistry at Solid Electrodes, Dekker, New York, 1969.
4 D.T. Sawyer and J.L. Roberts, Jr., Experimental Electrochemistry for Chemists, Wiley, New York, 1974.
5 A.J. Bard and L.R. Faulkner, Electrochemical Methods, Wiley, New York, 1980.
6 A. Weissberger and B.W. Rossiter (Eds.), Techniques of Chemistry, Vol. 1, Part IIA, Wiley Interscience, New York, 1971.
7 R. Greef, R. Peat, L.M. Peter, D. Pletcher and J. Robinson, Instrumental Methods in Electrochemistry, Wiley, New York, 1985.
8 A.J. Fry and W.E. Brilton, Topics in Organic Electrochemistry, Plenum, New York, 1986.
A.J. Fry, Synthetic Organic Electrochemistry, Harper and Row, New York, 1972.
9 M.M. Baizer, Organic Electrochemistry, Dekker, New York, 1973.
10 G. Dryhurst, Electrochemistry of Biological Molecules, Academic Press, New York, 1977.
11 D.T. Sawyer (Ed.), Electrochemical Studies of Biological Systems, ACS Symposium Series 38, American Chemical Society, Washington D.C., 1978.
12 Z. Nagy, Electrochemical Synthesis of Inorganic Compounds, Plenum, New York, 1985.
13 E.A. Seddon and K.R. Seddon, The Chemistry of Ruthenium, Elsevier, New York, 1984.
14 K.R. Seddon, Coord. Chem. Rev., 41 (1982) 79; 67 (1985) 171.
15 F.A. Cotton and G. Wilkinson, Advanced Inorganic Chemistry, 4th edn., Wiley, New York, 1980, pp. 912–933.
16 L.W. Niedrach and A.D. Tevebaugh, J. Am. Chem. Soc., 73 (1951) 2835.
17 J.A. Page and G. Wilkinson, J. Am. Chem. Soc., 74 (1952) 6149.
18 D.N. Hendrickson, Y.S. Sohn, W.H. Morrison, Jr., and H.B. Gray, Inorg. Chem., 11 (1972) 808.
19 D.D. DeFord and A.W. Davidson, J. Am. Chem. Soc., 73 (1951) 1469.
20 M.D. Silverman and H.A. Levy, J. Am. Chem. Soc., 76 (1954) 3319.
21 D.T. Sawyer, R.S. George and J.B. Bagger, J. Am. Chem. Soc., 81 (1959) 5893.
22 A. Sevcik, Collect. Czech. Chem. Commun., 13 (1948) 349.
23 R.R. Gagné, C.A. Koval and G.C. Lisensky, Inorg. Chem., 19 (1980) 2854.
24 J.N. Armor and M.Z. Hoffman, Inorg. Chem., 14 (1975) 444.
25 R.W. Callahan and T.J. Meyer, Inorg. Chem., 16 (1977) 574.
26 D.W. Pipes and T.J. Meyer, Inorg. Chem., 23 (1984) 2466.
27 K. Aoyagi, M. Mukaida, H. Kakihana and K. Shimizu, J. Chem. Soc., Dalton Trans., (1985) 1733.
28 A.A. Vlček, Coord. Chem. Rev., 43 (1982) 39.
29 J.A. McCleverty, Prog. Inorg. Chem., 10 (1968) 49.
30 R.P. Burns and C.A. McAuliffe, Adv. Inorg. Chem. Radiochem., 22 (1979) 303.
31 J. Miller and A.L. Balch, Inorg. Chem., 10 (1971) 1410.
32 K.W. Lam, K.E. Johnson and D.G. Lee, J. Electrochem. Soc., 125 (1978) 1069.
33 T.J. Meyer, J. Electrochem. Soc., 131 (1984) 221C.
34 S. Brownstein, G.A. Heath, A. Sengupta and D.A. Sharp, J. Chem. Soc., Chem. Commun., (1983) 669.
35 H. Taube, Surv. Prog. Chem., 6 (1973) 1.

36 J.F. Wishart, A. Bino and H. Taube, Inorg. Chem., 25 (1986) 3318.

37 D.S. Eggleston, K.A. Goldsby, D.J. Hodgson and T.J. Meyer, Inorg. Chem., 24 (1985) 4573.

38 A. Seal and S. Ray, Acta Crystallogr., Sect. C, 40 (1984) 929.

39 B.K. Ghosh, A. Mukhopadhyay, S. Goswami, S. Ray and A. Chakravorty, Inorg. Chem., 23 (1984) 4633.

40 K. Kalyanasundaram, Coord. Chem. Rev., 46 (1982) 159.

41 A. Juris, F. Barigelletti, S. Campagna, V. Balzani, P. Belser and A.V. Zelewsky, Coord. Chem. Rev., 84 (1988) 85.

42 N.E. Tokel-Takvoryan, R.W. Hemingway and A.J. Bard, J. Am. Chem. Soc., 95 (1973) 6582.

43 T. Saji and S. Aoyagui, J. Electroanal. Chem. Interfacial Electrochem., 58 (1975) 401.

44 C.M. Elliott and E.J. Hersheuhart, J. Am. Chem. Soc., 104 (1982) 7519.

45 Y. Ohsawa, M.K. DeArmond, K.W. Hanck and D.E. Morris, J. Am. Chem. Soc., 105 (1983) 6522.

46 J.G. Gaudiello, P.R. Sharp and A.J. Bard, J. Am. Chem. Soc., 104 (1982) 6373.

47 J.G. Gaudiello, P.G. Bradley, K.A. Norton, W.H. Woodruff and A.J. Bard, Inorg. Chem., 23 (1984) 3.

48 M.A. Weiner and A. Basu, Inorg. Chem., 19 (1980) 2797.

49 D.P. Rillema, G. Allen, T.J. Meyer and D. Conrad, Inorg. Chem., 22 (1983) 1617.

50 R.S. Glass and L.R. Faulkner, J. Phys. Chem., 85 (1981) 1160.

51 C.M. Elliott, R.A. Freitag and D.D. Balaney, J. Am. Chem. Soc., 107 (1985) 4647.

52 A. Ceulemans and L.G. Vanquickenborne, J. Am. Chem. Soc., 103 (1981) 2238.

53 B.P. Sullivan, D.J. Salmon and T.J. Meyer, Inorg. Chem., 17 (1978) 3334.

54 B.P. Sullivan, D.J. Salmon, T.J. Meyer and J. Peedin, Inorg. Chem., 18 (1979) 3369.

55 B.P. Sullivan, D. Conrad and T.J. Meyer, Inorg. Chem., 24 (1985) 3640.

56 D.E. Morris, K.W. Hanck and M.K. DeArmond, J. Am. Chem. Soc., 105 (1983) 3032.

57 Y. Ohsawa, M.K. DeArmond, K.W. Hanck and C.G. Moreland, J. Am. Chem. Soc., 107 (1985) 5383.

58 M.K. DeArmond, K.W. Hanck and D.W. Wertz, Coord. Chem. Rev., 64 (1985) 65.

59 R.J. Crutchley and A.B.P. Lever, Inorg. Chem., 21 (1982) 2276.

60 R.J. Crutchley, A.B.P. Lever and A. Poggi, Inorg. Chem., 22 (1983) 2647.

61 A.K.-D. Mesmaeker, R. Nasielski-Hinkens, D. Maetens, D. Pauwells and J. Nasielski, Inorg. Chem., 23 (1984) 377.

62 M.N. Ackermann and L.V. Interrante, Inorg. Chem., 23 (1984) 3904.

63 A. Juris, F. Barigelletti, V. Balzani, P. Belser and A.V. Zelewsky, Inorg. Chem., 24 (1985) 202.

64 K.J. Brewer, W.R. Murphy, Jr., S.R. Spurlin and J.D. Petersen, Inorg. Chem., 25 (1986) 882.

65 D.P. Rillema, D.G. Taghdiri, D.S. Jones, C.D. Keller, L.A. Worl, T.J. Meyer and H.A. Levy, Inorg. Chem., 26 (1987) 578.

66 C.A. Goss and H.D. Abruña, Inorg. Chem., 24 (1985) 4263.

67 A. Juris, P. Belser, F. Barigelletti, A.V. Zelewsky and V. Balzani, Inorg. Chem., 25 (1986) 256.

68 J.L. Sadler and A.J. Bard, J. Am. Chem. Soc., 90 (1968) 1979.

69 J.R. Kuder, P.J. Cressman, F.D. Saeva, D. Wychick and G.C. Hartmann, J. Chem. Phys., 61 (1974) 2740.

70 R.O. Loutfy and J.H. Sharp, J. Am. Chem. Soc., 99 (1977) 4049.

71 S. Goswami, R.N. Mukherjee and A. Chakravorty, Inorg. Chem., 22 (1983) 2825.

72 A.K. Mahapatra, S. Datta, S. Goswami, M. Mukherjee, A.K. Mukherjee and A. Chakravorty, Inorg. Chem., 25 (1986) 1715.
73 G.K. Lahiri, S. Bhattacharya, M. Mukherjee, A.K. Mukherjee and A. Chakravorty, Inorg. Chem., 26 (1987) 3359.
74 A.R. Chakravarty and A. Chakravorty, Inorg. Chem., 20 (1981) 3138.
75 A.R. Chakravarty, A. Chakravorty, F.A. Cotton, L.R. Falvello, B.K. Ghosh and M. Tomas, Inorg. Chem., 22 (1983) 1892.
76 A.R. Chakravarty and A. Chakravorty, J. Chem. Soc., Dalton Trans., (1983) 961.
77 S. Goswami, A.R. Chakravarty and A. Chakravorty, Inorg. Chem., 20 (1981) 2246.
78 S. Goswami, A.R. Chakravarty and A. Chakravorty, Inorg. Chem., 21 (1982) 2737.
79 S. Goswami, A.R. Chakravarty and A. Chakravorty, J. Chem. Soc., Chem. Commun., (1982) 1288.
80 S. Goswami, A.R. Chakravarty and A. Chakravorty, Inorg. Chem., 22 (1983) 602.
81 P. Ghosh and A. Chakravorty, J. Chem. Soc., Dalton Trans., (1985) 361.
82 R.A. Krause and K. Krause, Inorg. Chem., 19 (1980) 2600.
83 R.A. Krause and K. Krause, Inorg. Chem., 21 (1982) 1714.
84 R.A. Krause and K. Krause, Inorg. Chem., 23 (1984) 2195.
85 S. Wolfang, T.C. Strekas, H.D. Gafney, R.A. Krause and K. Krause, Inorg. Chem., 23 (1984) 2650.
86 P. Ghosh and A. Chakravorty, Inorg. Chem., 23 (1984) 2242.
87 E.S. Dodsworth and A.B.P. Lever, Chem. Phys. Lett., 119 (1985) 61.
88 E.S. Dodsworth and A.B.P. Lever, Chem. Phys. Lett., 124 (1986) 152.
89 A.L. Balch and R.H. Holm, J. Am. Chem. Soc., 88 (1966) 5201.
90 L.F. Warren, Inorg. Chem., 16 (1977) 2814.
91 P. Belser, A.V. Zelewsky and M. Zehnder, Inorg. Chem., 20 (1981) 3098.
92 K. Rieder, U. Hauser, H. Siegenthaler, E. Schmidt and A. Ludi, Inorg. Chem., 14 (1975) 1902.
93 S. Joss, H. Reust and A. Ludi, J. Am. Chem. Soc., 103 (1981) 981.
94 L. Pasimeni, M. Brustolon and C. Corvaja, J. Magn. Reson., 21 (1976) 259.
95 S. Patai (Ed.), The Chemistry of the Quinoid Compounds, Parts 1 and 2, Wiley, New York, 1974.
96 R.H. Thompson, Naturally Occurring Quinones. III Recent Advances, Chapman and Hall, London, 1987.
97 M.D. Stallings, M.M. Morrison and D.T. Sawyer, Inorg. Chem., 20 (1981) 2655.
98 C.G. Pierpont and R.M. Buchanan, Coord. Chem. Rev., 38 (1981) 45.
99 S.E. Jones, L.E. Leon and D.T. Sawyer, Inorg. Chem., 21 (1982) 3692, and references therein.
100 D.J. Gordon and R.F. Fenske, Inorg. Chem., 21 (1982) 2907, 2916, and references therein.
101 A.Y. Girgis, Y.S. Sohn and A.L. Balch, Inorg. Chem., 14 (1975) 2327.
102 N.G. Connelly, I. Manners, J.R.C. Protheroe and M.W. Whiteley, J. Chem. Soc., Dalton Trans., (1984) 2713.
103 S.D. Pell, R.B. Salmonsen, A. Abelleira and M.J. Clarke, Inorg. Chem., 23 (1984) 385.
104 M.-A. Haga, E.S. Dodsworth and A.B.P. Lever, Inorg. Chem., 25 (1986) 447.
105 M.-A. Haga, E.S. Dodsworth, A.B.P. Lever, S.R. Boone and C.G. Pierpont, J. Am. Chem. Soc., 108 (1986) 7413.
106 S.R. Boone and C.G. Pierpont, Inorg. Chem., 26 (1987) 1769.
107 E.C. Slater (Ed.), Flavins and Flavoproteins, Elsevier, New York, 1966.
108 P. Hemmerich, V. Massey, H. Michel and C. Schug, Struct. Bonding (Berlin), 48 (1982) 93.

109 J.G. Mohanty and A. Chakravorty, Inorg. Chem., 15 (1976) 2912; 16 (1977) 1561.
110 M. Wang and C.J. Fritchie, Jr., Acta Crystallogr. Sect. B, 29 (1973) 2040.
111 R. Norrestam and M.V. Glehn, Acta Crystallogr. Sect. B, 28 (1972) 434.
112 R. Norrestam and B. Stensland, Acta Crystallogr. Sect. B, 28 (1972) 440.
113 M.J. Clarke, M.G. Dowling, A.R. Garafalo and T.F. Brennan, J. Biol. Chem., 255 (1980) 3472.
114 D.A. Dixon, D.L. Linder, B. Branchaud and W.N. Lipscomb, Biochemistry, 18 (1979) 5770.
115 A. Ehrenberg, L.E.G. Eriksson and F. Müller, in E.C. Slater (Ed.), Flavins and Flavoproteins, Elsevier, New York, 1966, p. 37.
116 A. Ehrenberg, F. Müller and P. Hemmerich, Eur. J. Biochem., 2 (1967) 286.
117 B. Janik and P.J. Elving, Chem. Rev., 68 (1968) 295.
118 G. Dryhurst, Electrochemistry of Biological Molecules, Academic Press, New York, 1977, Chapt. 7.
119 S.V. Tatwawadi, K.S. Santhanam and A.J. Bard, J. Electroanal. Chem. Interfacial Electrochem., 17 (1968) 411.
120 D.T. Sawyer and R.L. McCreery, Inorg. Chem., 11 (1972) 779.
121 P. Hemmerich and J. Spence, in E.C. Slater (Ed.), Flavins and Flavoproteins, Elsevier, New York, 1966, p. 82.
122 M.J. Clarke, M.G. Dowling, A.R. Garafalo and T.F. Brennan, J. Am. Chem. Soc., 101 (1979) 223.
123 M.J. Clarke and M.G. Dowling, Inorg. Chem., 20 (1981) 3506.
124 M.G. Dowling and M.J. Clarke, Inorg. Chim. Acta, 78 (1983) 153.
125 J.-H. Fuhrhop, Struct. Bonding (Berlin), 18 (1974) 1.
126 D.W. Clack and N.S. Hush, J. Am. Chem. Soc., 87 (1965) 4238.
127 R.H. Felton and H. Linschitz, J. Am. Chem. Soc., 88 (1966) 1113.
128 A. Wolberg and J. Manassen, J. Am. Chem. Soc., 92 (1970) 2982.
129 J. Fajer, D.C. Borg, A. Forman, D. Dolphin and R.H. Felton, J. Am. Chem. Soc., 92 (1970) 3451.
130 A. Stanienda and G. Biebl, Z. Phys. Chem. (Frankfurt am Main), 52 (1967) 254.
131 J.-H. Fuhrhop, K.M. Kadish and D.G. Davis, J. Am. Chem. Soc., 95 (1973) 5140.
132 K.M. Kadish and M.M. Morrison, J. Am. Chem. Soc., 98 (1976) 3326.
133 K.M. Kadish, D.G. Davis and J.-H. Fuhrhop, Angew. Chem., 84 (1972) 1072.
134 P.J. Brothers and J.P. Collman, Acc. Chem. Res., 19 (1986) 209.
135 E.B. Fleischer, R. Thorp and D. Venerable, J. Chem. Soc., Chem. Commun., (1969) 475.
136 B.C. Chow and I.A. Cohen, Bioinorg. Chem., 1 (1971) 57.
137 M. Tsutsui, D. Ostfeld and L.M. Hoffman, J. Am. Chem. Soc., 93 (1971) 1820.
138 G.W. Sovocool, F.R. Hopf and D.G. Whitten, J. Am. Chem. Soc., 94 (1972) 4350.
139 A. Antipas, J.W. Buchler, M. Gouterman and P.D. Smith, J. Am. Chem. Soc., 100 (1978) 3015.
140 M. Barley, J.Y. Becker, G. Domazetis, D. Dolphin and B.R. James, Can. J. Chem., 61 (1983) 2389.
141 J.P. Collman, C.E. Barnes, T.J. Collins and P.J. Brothers, J. Am. Chem. Soc., 103 (1981) 7030.
142 H. Masuda, T. Taga, K. Osaki, H. Sugimoto, M. Mori and H. Ogoshi, J. Am. Chem. Soc., 103 (1981) 2199.
143 H. Sugimoto, T. Higashi, M. Mori, M. Nagano, Z.-I. Yoshida and H. Ogoshi, Bull. Chem. Soc. Jpn., 55 (1982) 822.
144 J.P. Collman, C.E. Barnes, P.J. Brothers, T.J. Collins, T. Ozawa, J.C. Gallucci and J.A. Ibers, J. Am. Chem. Soc., 106 (1984) 5151.

145 J.J. Bonnet, S.S. Eaton, G.R. Eaton, R.H. Holm and J.A. Ibers, J. Am. Chem. Soc., 95 (1973) 2141.
146 R.G. Little and J.A. Ibers, J. Am. Chem. Soc., 95 (1973) 8583.
147 J.P. Collman, C.E. Barnes, P.N. Swepston and J.A. Ibers, J. Am. Chem. Soc., 106 (1984) 3500.
148 J.P. Collman, C.E. Barnes and L.K. Woo, Proc. Natl. Acad. Sci. U.S.A., 80 (1983) 7684.
149 G.M. Brown, F.R. Hopf, J.A. Ferguson, T.J. Meyer and D.G. Whitten, J. Am. Chem. Soc., 95 (1973) 5939.
150 G.M. Brown, F.R. Hopf, T.J. Meyer and D.G. Whitten, J. Am. Chem. Soc., 97 (1975) 5385.
151 D.P. Rillema, J.K. Nagle, L.F. Barringer, Jr., and T.J. Meyer, J. Am. Chem. Soc., 103 (1981) 56.
152 M. Barley, J.Y. Becker, G. Domazetis, D. Dolphin and B.R. James, J. Chem. Soc., Chem. Commun., (1981) 982.
153 K.M. Kadish and D. Chang, Inorg. Chem., 21 (1982) 3614.
154 K.M. Kadish, D.J. Legglett and D. Chang, Inorg. Chem., 21 (1982) 3618.
155 T. Malinski, D. Chang, L.A. Bottomley and K.M. Kadish, Inorg. Chem., 21 (1982) 4248.
156 S.S. Eaton, G.R. Eaton and R.H. Holm, J. Organomet. Chem., 39 (1972) 179.
157 J.T. Groves and R. Quinn, Inorg. Chem., 23 (1984) 3844.
158 J.P. Collman, J.W. Prodolliet and C.R. Leidner, J. Am. Chem. Soc., 108 (1986) 2916.
159 J.P. Collman, K. Kim and C.R. Leidner, Inorg. Chem., 26 (1987) 1152.
160 A.B.P. Lever, The Phthalocyanine, Adv. Inorg. Chem. Radiochem., 7 (1965) 27.
161 L.J. Boucher, in G.A. Melson (Ed.), Coordination Chemistry of Macrocyclic Compounds, Plenum, New York, 1979, p. 461.
162 K. Kasuga and M. Tsutsui, Coord. Chem. Rev., 32 (1980) 67.
163 D.L. Ledson and M.V. Twigg, Inorg. Chim. Acta, 13 (1975) 43.
164 A.B.P. Lever and J.P. Wilshire, Can. J. Chem., 54 (1976) 2514.
165 D.W. Clack, N.S. Hush and L.S. Woolsey, Inorg. Chim. Acta, 19 (1976) 129.
166 L.D. Rollmann and R.T. Iwamoto, J. Am. Chem. Soc., 90 (1968) 1455.
167 P.C. Krueger and M.E. Kenney, J. Inorg. Nucl. Chem., 25 (1963) 303.
168 B.D. Berezin and G.V. Sennikova, Dokl. Akad. Nauk SSSR, 159 (1964) 117.
169 I.M. Keen and B.W. Malerbi, J. Inorg. Nucl. Chem., 27 (1965) 1311.
170 N.P. Farrell, A.J. Murray, J.R. Thornback, D.H. Dolphin and B.R. James, Inorg. Chim. Acta, 28 (1978) L144.
171 C.K. Choy, J.R. Mooney and M.E. Keeney, J. Magn. Reson., 35 (1979) 1.
172 S. Omiya, M. Tsutsui, E.F. Meyer, Jr., I. Bernal and D.L. Cullen, Inorg. Chem., 19 (1980) 134.
173 L.J. Boucher and P. Rivera, Inorg. Chem., 19 (1980) 1816.
174 M.M. Doeff and D.A. Sweigart, Inorg. Chem., 20 (1981) 1683.
175 D. Dolphin, B.R. James, A.J. Murray and J.R. Thornback, Can. J. Chem., 58 (1980) 1125.
176 G.J. Ferraudi and D.R. Prasad, J. Chem. Soc., Dalton Trans., (1984) 2137.